Mass hierarchy, 2-3 mixing and CP-phase with Huge Atmospheric Neutrino Detectors

E. Kh. Akhmedov,[1,*] Soebur Razzaque,[2,†] and A. Yu. Smirnov[3,‡]

¹Max-Planck-Institut fur Kernphysik,

Saupfercheckweg 1, D-69117 Heidelberg, Germany

²School of Physics, Astronomy and Computational Sciences,

George Mason University, Fairfax, VA 22030, USA

³The Abdus Salam International Centre for Theoretical Physics, I-34100 Trieste, Italy

(Dated: April 29, 2013)

Abstract

We explore the physics potential of multi-megaton scale ice or water Cherenkov detectors with low (~ 1 GeV) threshold. Using some proposed characteristics of the PINGU detector setup we compute the distributions of events versus neutrino energy E_ν and zenith angle θ_z, and study their dependence on yet unknown neutrino parameters. The ($E_\nu - \theta_z$) regions are identified where the distributions have the highest sensitivity to the neutrino mass hierarchy, to the deviation of the 2-3 mixing from the maximal one and to the CP-phase. We evaluate significance of the measurements of the neutrino parameters and explore dependence of this significance on the accuracy of reconstruction of the neutrino energy and direction. The effect of degeneracy of the parameters on the sensitivities is also discussed. We estimate the characteristics of future detectors (energy and angle resolution, volume, etc.) required for establishing the neutrino mass hierarchy with high confidence level. We find that the hierarchy can be identified at 3σ – 10σ level (depending on the reconstruction accuracies) after 5 years of PINGU operation.

PACS numbers: 14.60.Pq, 14.60.St

---

*Also at the National Research Centre Kurchatov Institute, Moscow, Russia.; Electronic address: akhmedov@mpi-hd.mpg.de

†Present address: Department of Physics, University of Johannesburg, C1-Lab 140, PO Box 524, Auckland Park 2006, South Africa.; Electronic address: srazzaque@uj.ac.za

‡Electronic address: smirnov@ictp.it

I. INTRODUCTION

Atmospheric neutrino studies have enormous physics potential which has not been fully explored yet. Atmospheric neutrinos can be used (i) to explore different effects of neutrino propagation: oscillations in vacuum and in matter, MSW resonance of neutrino oscillations [1, 2], as well as parametric enhancement effects [3], *etc.*; (ii) to determine neutrino oscillation parameters: mass squared differences, mixing angles, CP violation effects, mass hierarchy; (iii) to search for new physics beyond the standard framework with 3 light neutrinos: new neutrino states, non-standards interactions, violation of fundamental symmetries, *etc.*; (iv) to perform, in principle, the oscillation tomography of the Earth.

Among major results obtained with the atmospheric neutrinos are the discovery of neutrino oscillations [4], first measurements of θ_{23} and Δm_{32}^2 [5] and various bounds on new physics [6].

The physics potential of atmospheric neutrino studies with existing and forthcoming experiments has been widely discussed before (see, e.g., [7] and references therein). In particular, the potential of the IceCube's DeepCore (the currently existing detector within the inner core of IceCube with an energy threshold $E_\nu \sim 10$ GeV [8]) for studying neutrino oscillations has been explored in Refs. [9–11]. The first experimental results on atmospheric neutrino oscillations in DeepCore have been reported in Ref. [12].

Although at the probability level the effects of the neutrino mass hierarchy, deviation of the 2-3 mixing from the maximal one, and CP-violation in specific oscillation channels can be of order 1, there are a number of factors which substantially reduce the effects at the level of observable events. As a result, determination of the neutrino parameters becomes difficult if possible at all. The main challenges include (1) relatively low statistics, especially at energies above a few GeV; (2) the presence of both neutrinos and antineutrinos in the original neutrino flux and the difficulty of experimental separation of the signals from neutrinos and antineutrinos, especially in large (megaton scale) detectors; (3) the existence of both ν_e and ν_μ in the original fluxes; (4) a significant smearing of the signal over the energies and zenith angles, related to large uncertainties in reconstruction of the neutrino energy and direction.

Recently, the idea has been entertained that large statistics of events that can be collected over a wide energy range in multi-megaton detectors with low (a few GeV) thresh-

olds, supplemented by relatively mild technological improvements, can alleviate or remove the above-mentioned shortcomings [13–15]. High statistics will allow one to make specific selections of events with different geometries from certain ranges of energies and zenith angles in order to enhance the sensitivity of the experiment to various neutrino parameters, to resolve degeneracies between those parameters, and to reduce the effects of uncertainties of the input parameters (such as the neutrino fluxes and experimental resolutions). Recent considerations and discussions of the multi-megaton ice detector PINGU (the proposed upgrade of the IceCube detector) [16] show that this hope may actually be realized.

In this paper we explore the possibilities of studying the neutrino parameters in multi-megaton scale ice or water Cherenkov detectors with energy thresholds as low as a few GeV. We study the energy and zenith angle distributions of events and their dependence on the neutrino mass hierarchy (ordering), the deviation of the 2-3 mixing from the maximal one and on the CP-phase. We identify the geometry of the events and the kinematic regions in the $(E_\nu - \cos\theta_z)$ plane where the dependence on a specific neutrino parameter is maximal. We compute significance of measurements of these parameters and explore dependence of the significance on the energy and zenith angle resolutions of the detector, i.e. on the accuracy of reconstruction of the neutrino energy and direction.

In our calculations we use some provisional characteristics of the PINGU detector, in particular the effective volume and its energy dependence. At the same time, we perform our analysis with an effort to make it as much as possible independent of specific experimental features, which are yet to be determined.

The paper is organized as follows. In sec. II we summarize relevant information about the oscillation probabilities. In Sec. III we present distributions of events in the $E_\nu - \cos\theta_z$ plane as well as significance plots for determination of various neutrino parameters. In sec. IV we perform smearing of the event densities using neutrino energy and direction reconstruction functions. In this section we also study dependence of the significance of the determination of the neutrino mass hierarchy on the energy and angular resolutions (the widths of the reconstruction functions) of the detector. In addition, we discuss here the issue of degeneracy of neutrino parameters. Sec. V contains discussion of our results and conclusions.

II. OSCILLATION PROBABILITIES

In this section we discuss dependence of the oscillation probabilities on the neutrino mass hierarchy and on the deviation of the 2-3 mixing from the maximal one. We consider the evolution of three neutrino flavors $\nu_f \equiv (\nu_e, \nu_\mu, \nu_\tau)^T$ in the propagation basis, $\nu_{prop} = (\nu_e, \tilde{\nu}_2, \tilde{\nu}_3)^T$, defined as $\nu_f = U_{23} I_\delta \nu_{prop}$. We use the standard parameterization of the PMNS mixing matrix, $U_{PMNS} = U_{23} I_\delta U_{13} U_{12}$, where U_{ij} is the matrix of rotations in the $ij-$ plane and $I_\delta = diag(1, 1, e^{i\delta})$ is the matrix with CP-violating phase.

We consider the neutrino energy range $E_\nu > (2-3)$ GeV which includes the 1-3 resonances and parametric enhancement ridges, and where the sensitivity to the neutrino mass hierarchy is expected to be maximal. Also in this range one expects small CP-violation effects, so that their degeneracy with the effects of the mass hierarchy is small. In this energy range we can neglect the effects of 1-2 mixing and mass splitting in the first approximation. Then the oscillation probabilities can be written in the following forms, which are convenient for discussion of the neutrino mass hierarchy [17]:

$$P_{ee} = 1 - P_A \,, \tag{1}$$

$$P_{\mu e} = P_{e\mu} = s_{23}^2 P_A \,, \tag{2}$$

$$P_{e\tau} = c_{23}^2 P_A \,, \tag{3}$$

$$P_{\mu\mu} = 1 - \frac{1}{2}\sin^2 2\theta_{23} - s_{23}^4 P_A + \frac{1}{2}\sin^2 2\theta_{23}\sqrt{1 - P_A}\cos\phi_X, \tag{4}$$

$$P_{\mu\tau} = \frac{1}{2}\sin^2 2\theta_{23} - s_{23}^2 c_{23}^2 P_A - \frac{1}{2}\sin^2 2\theta_{23}\sqrt{1 - P_A}\cos\phi_X, \tag{5}$$

where $P_A \equiv |A_{e\tilde{3}}|^2$ and

$$\phi_X \equiv arg[A_{\tilde{2}\tilde{2}} A_{\tilde{3}\tilde{3}}^*].$$

Here A_{ij} are the amplitudes of $\tilde{\nu}_i \rightarrow \tilde{\nu}_j$ transitions between the states of the propagation basis. From these formulas one immediately sees correlations between different probabilities. The amplitudes can be represented as

$$A_{\tilde{3}\tilde{3}} = |A_{\tilde{3}\tilde{3}}|e^{i\phi_{33}} = \sqrt{1 - P_A}e^{i\phi_{33}}, \qquad A_{\tilde{2}\tilde{2}} = e^{i\phi_{22}},$$

so that $\phi_X = \phi_{22} - \phi_{33}$.

In the case of neutrino propagation in matter of constant density we obtain explicitly

$$\phi_X = \arctan\left(\cos 2\theta_{13}^m \tan\frac{\phi_{31}^m}{2}\right) + \frac{V + \Delta}{2}x,$$

where

$$\cos 2\theta_{13}^m = \frac{\cos 2\theta_{13}\Delta - V}{\sqrt{(\cos 2\theta_{13}\Delta - V)^2 + \Delta^2 \sin^2 2\theta_{13}}},$$

$$\phi_{31}^m = x\sqrt{(\cos 2\theta_{13}\Delta - V)^2 + \Delta^2 \sin^2 2\theta_{13}}$$

and

$$\Delta \equiv \frac{\Delta m_{31}^2}{2E_\nu}.$$

For matter of constant density

$$P_A = \sin^2 2\theta_{13}^m \sin^2 \frac{\phi_{31}^m}{2}.$$

In the limit $\theta_{13} \to 0$, we obtain

$$\phi_X \approx \phi_{32} \equiv \frac{\Delta m_{32}^2 x}{2E}. \tag{6}$$

At the MSW resonance, $\tan^2 \theta_{13}^m = 1$, and the phase ϕ_X is again given by (6) (up to a factor $\cos^2 \theta_{13} \approx 1$). The phase ϕ_X approximately equals ϕ_{32} also at energies far above the resonance energy and coincides with ϕ_{32} in vacuum. Eq. (6) is therefore violated only in the resonance region, except at the resonance point itself. This is a consequence of the smallness of the mixing angle θ_{13}.

The probabilities for antineutrino channels can be obtained from the expressions in eqs. (1 - 5) by substituting $P_A \to \bar{P}_A$ and $\phi_X \to \bar{\phi}_X$, where

$$\bar{P}_A = P_A(V \to -V), \quad \bar{\phi}_X = \phi_X(V \to -V).$$

In the case of normal mass hierarchy (NH), the 1-3 antineutrino mixing in matter is suppressed, consequently, $\bar{P}_A \approx 0$ and ϕ_X nearly equals the vacuum phase difference (6).

In the approximation of zero 1-2 splitting, for the inverted neutrino mass hierarchy (IH) we obtain

$$P_A^{IH} = \bar{P}_A^{NH}, \quad \phi_X^{IH} = -\bar{\phi}_X^{NH},$$

where $\bar{\phi}_X^{NH} = \phi_X^{NH}(V \to -V)$ (see the Appendix). Therefore

$$P_{\alpha\beta}^{IH} = \bar{P}_{\alpha\beta}^{NH}, \quad \bar{P}_{\alpha\beta}^{IH} = P_{\alpha\beta}^{NH}. \tag{7}$$

The equalities in eq. (7) receive corrections from non-zero 1-2 mass splitting and mixing.

The information about the neutrino mass hierarchy is encoded mainly in P_A and also in ϕ_X. If $P_A = 0$ and $\phi_X = \phi_{32}$, the oscillation probabilities for the IH and NH coincide.
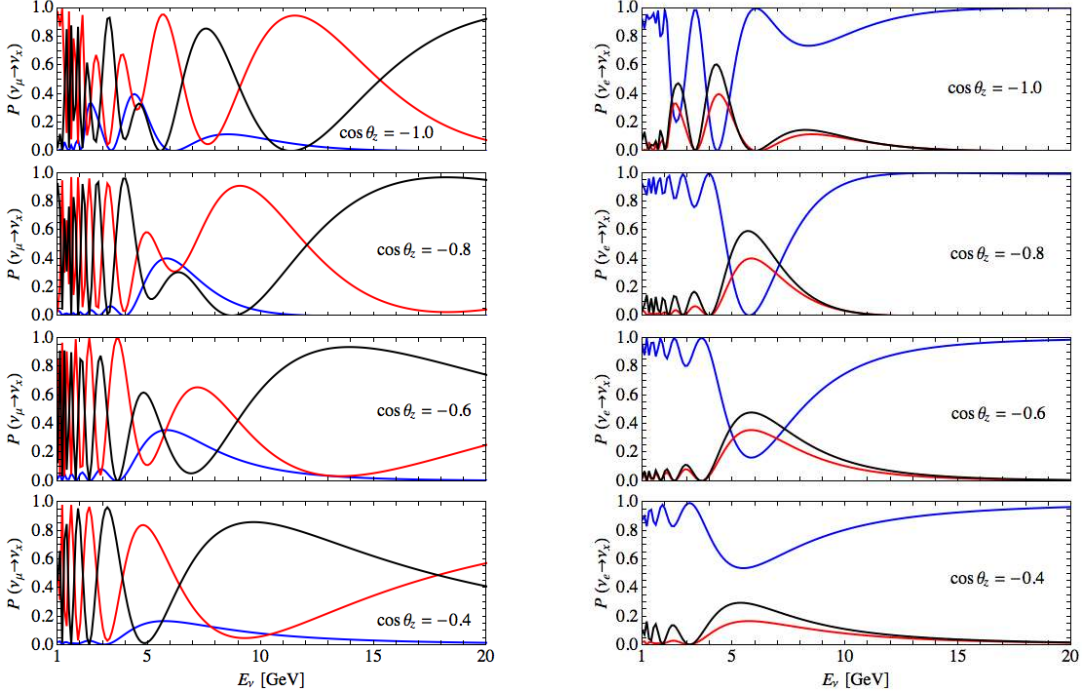
FIG. 1: Dependence of the oscillation probabilities in various channels on neutrino energy for a number of values of the zenith angle. Normal mass hierarchy is assumed. Left panel is for the $\nu_\mu \to \nu_x$ channels, and right panel is for the $\nu_e \to \nu_x$ channels, where $\nu_x = \nu_e$ (blue lines), ν_μ (red lines) and ν_τ (black lines). We use the values of the neutrino parameters defined in the text and $\delta = 0$.

Let us consider in more detail eq. (4) for the probability $P_{\mu\mu}$, which plays a crucial role in our analysis (a similar analysis can be performed for $P_{\mu\tau}$ as well.) The first two terms in (4) correspond to $\bar{P}$, the average 2ν probability with vacuum oscillation depth, which is due to 2-3 mixing. The probability P_A is an oscillatory function of the neutrino energy (and the zenith angle), but in the resonance region the period of oscillations is determined by the oscillation length in matter $l_{13}^m \approx l_{23}/\sin 2\theta_{13} \approx (3 - 4)l_{23}$, which is much larger than the oscillation length l_{23} responsible for ϕ_X. The effects of the 1-3 mixing (and therefore the matter effects) (i) reduce the average probability, the third term in (4); (ii) reduce the depths of oscillations by the factor $\sqrt{1 - P_A}$, the fourth term in (4); and (iii) change the oscillation phase $\phi_{32} \to \phi_X$. The third and fourth terms lead to a change of the depths of the oscillations. These features are well seen in Fig. 1, where we show the dependence of the oscillation probabilities in various neutrino channels on the neutrino energy for different
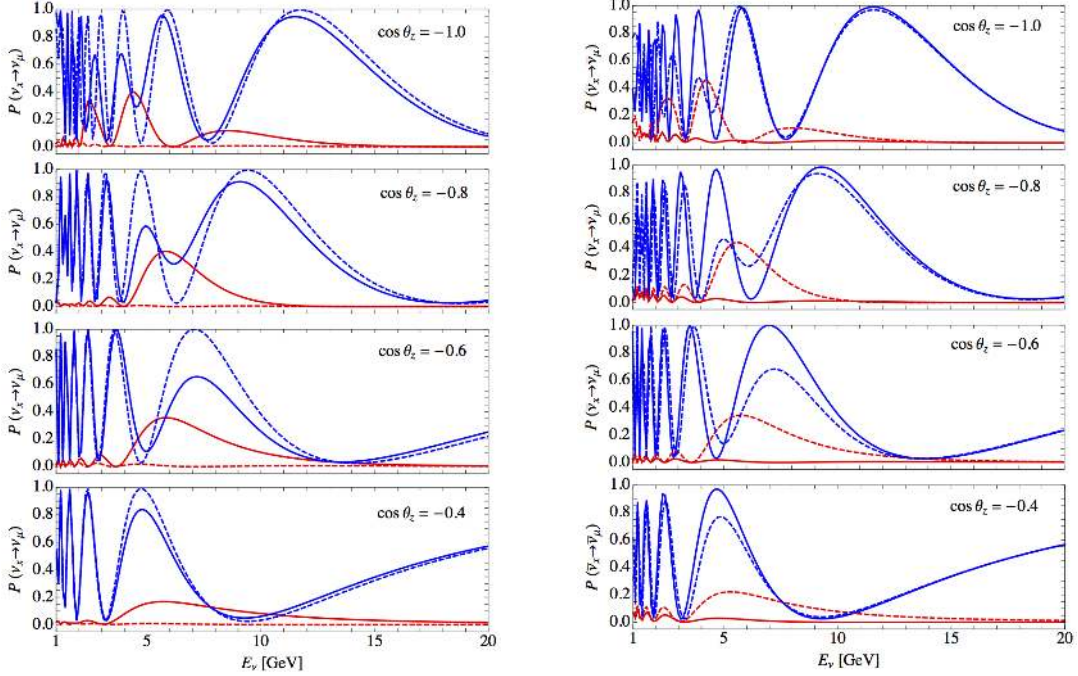
6

FIG. 2: Probabilities of oscillations of neutrinos of various flavors (blue lines for ν_μ, red lines for ν_e) to ν_μ vs. neutrino energy for a number of values of the zenith angle. The solid and dashed lines are for NH and IH, respectively. Left panel is for neutrinos, and right panel is for antineutrinos. All the parameters are the same as in Fig. 1.

values of the zenith angle. Figure 2 shows the oscillation probabilities for both the neutrino and antineutrino channels and for the two mass hierarchies.

We use the values of the neutrino parameters $\Delta m_{32}^2 = 2.35 \cdot 10^{-3}$ eV^2, $\Delta m_{21}^2 = 7.6 \cdot 10^{-5}$ eV^2, $\sin^2 \theta_{23} = 0.42$, $\sin^2 \theta_{12} = 0.312$ and $\sin^2 \theta_{13} = 0.025$, which are close to the current best fit values [18], and the PREM density profile of the Earth [19] for numerical computations.

The strongest modifications of the oscillation probabilities due to matter effects are in the resonance region $E_\nu \sim (4 - 8)$ GeV, where P_A has a peak due to the MSW resonance in the mantle of the Earth. For the selected values of the oscillation parameters the maximum of the peak is at $E_\nu = 6.2$ GeV and $\cos \theta_z = -0.68$. In addition, at this point the oscillation phase $\phi_{31}^m = \pi$. In the region $|\cos \theta_z| > 0.83$ and $E_\nu < 7$ GeV strong modifications of the oscillation probabilities are due to the parametric enhancement of the oscillations for the neutrino trajectories crossing the Earth's core, and also due to the MSW resonance in the core [13, 14]. Notice that $P_{\mu\mu}$, and consequently the mass hierarchy effects, strongly depend on the 2-3 mixing: the probability P_A enters $P_{\mu\mu}$ with the factor s_{23}^4.
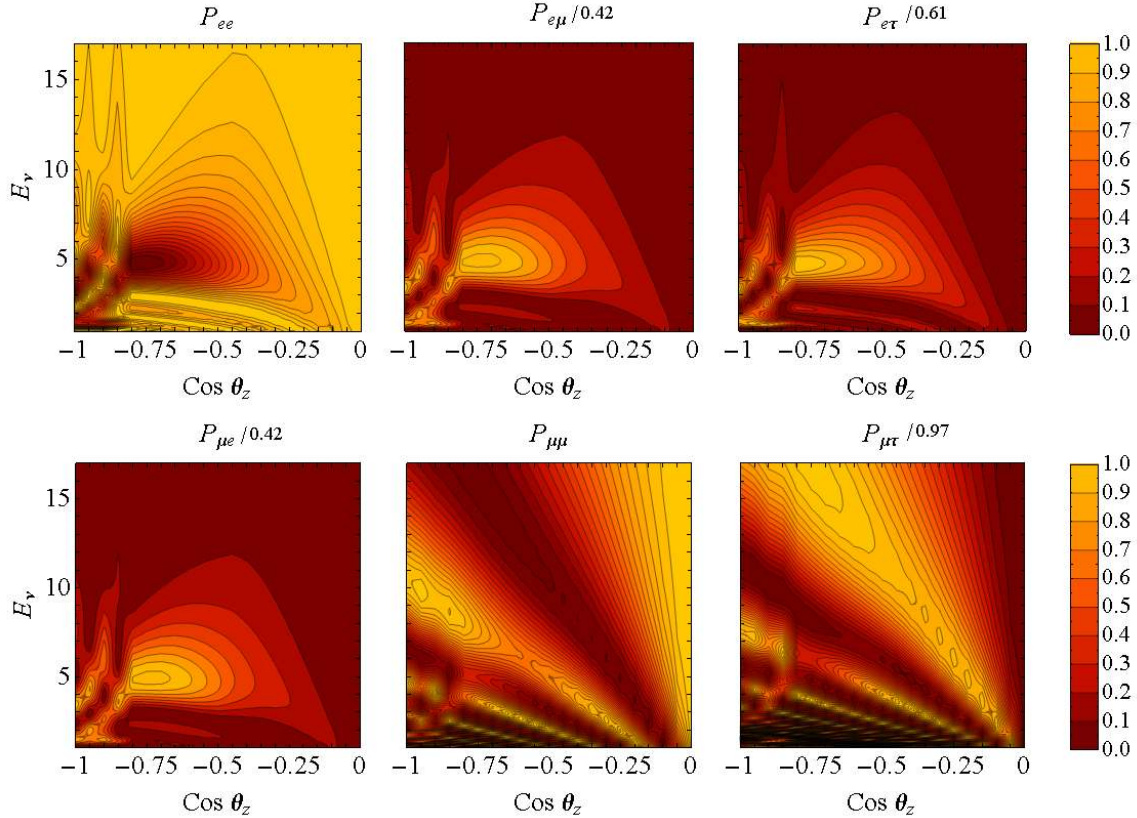
FIG. 3: Neutrino oscillograms of the Earth (lines of equal probabilities in the $E_\nu - \cos\theta_z$ plane) for different oscillation channels and for the values of the oscillation parameters indicated in the text. Shown are the oscillation probabilities normalized by their maximal values in the parameter space of the panels: $P_{\alpha,\beta}/P_{\alpha,\beta}^{max}$, with $P_{ee}^{max} = P_{\mu\mu}^{max} = 1$. E_ν is in GeV. Normal mass hierarchy is assumed.

In Fig. 3 we show the neutrino oscillograms – curves of equal oscillation probability in the $(E_\nu - \cos\theta_z)$ plane – for the $\nu_\mu \to \nu_x$ and $\nu_e \to \nu_x$ channels. The probabilities increase monotonically from darker-shaded to lighter-shaded regions.

III. NUMBERS OF EVENTS IN THE NEUTRINO ENERGY AND ZENITH AN-GLE PLANE

We consider first the numbers of events of different types produced by neutrinos with energies and zenith angles in small bins $\Delta(E_\nu)$ and $\Delta(\cos\theta_z)$. These would correspond to real observables if the neutrino energy and zenith angle could be reconstructed from

the measurements with negligible errors. In the next section we will study the effects of smearing of these distributions due to uncertainties of the neutrino energy and zenith angle reconstructions.

A.   Distributions of the ν_μ-like events

The ν_μ-like events (tracks) correspond to interactions $\nu_\mu + N \to \mu + X$, $\bar{\nu}_\mu + N \to \mu^+ + X$. There are also some contributions from ν_τ which produce τ with subsequent decay into μ. The number of ν_μ-like events in the ij-bin is

$$N_{ij,\mu}^{\mathrm{NH}} = 2\pi N_A \rho T \int_{\Delta_i \cos\theta_z} d\cos\theta_z \int_{\Delta_j E_\nu} dE_\nu \; V_{\mathrm{eff}}(E_\nu) D_\mu(E_\nu, \theta_z), \tag{8}$$

where T is the exposure time, N_A is the Avogadro's number, ρ is the density of ice, V_{eff} is the effective volume of the detector, and the number density of events per unit time per target nucleon is given by

$$D_\mu(E_\nu, \theta_z) = \left[\sigma^{CC} \left(\Phi_\mu^0 P_{\mu\mu} + \Phi_e^0 P_{e\mu} \right) + \bar{\sigma}^{CC} \left(\bar{\Phi}_\mu^0 \bar{P}_{\mu\mu} + \bar{\Phi}_e^0 \bar{P}_{e\mu} \right) \right]. \tag{9}$$

Here $\Phi_\alpha^0 = \Phi_\alpha^0(E_\nu, \theta_z)$, are the original fluxes of neutrinos ν_α. We use the effective volume of PINGU with 20 strings [20] which can be parameterized as

$$\rho V_{\mathrm{eff}}(E_\nu) = 14.6 \times [\log(E_\nu/\mathrm{GeV})]^{1.8} \; \mathrm{Mt}. \tag{10}$$

The volume increases from 2 Mt at $E_\nu = 2$ GeV to 20 Mt at $E_\nu = 20$ GeV. (In general V_{eff} depends also on θ_z.) We have found P_A and the probabilities $P_{\alpha\beta} = P_{\alpha\beta}(E_\nu, \theta_z)$ by performing numerical integration of the evolution equation for the complete $3\nu-$system. We use the deep inelastic cross-sections

$$\sigma^{CC}(E_\nu) = 7.30 \cdot 10^{-39}(E_\nu/\mathrm{GeV}) \; \mathrm{cm}^2,$$
$$\bar{\sigma}^{CC}(E_\nu) = 3.77 \cdot 10^{-39}(E_\nu/\mathrm{GeV}) \; \mathrm{cm}^2,$$

and we take the cross sections for electron and muon neutrinos of the same energy to be the same. In our calculations we use the Honda et al. atmospheric neutrino fluxes [21], which were calculated for the Kamioka site; however, for neutrino energies above a few GeV these should also give good approximations for the fluxes at the South Pole.

The fine-binned distribution of events (8) with $\Delta(\cos\theta_z) = 0.025$ and $\Delta E_\nu = 0.5$ GeV is shown in Fig. 4. The number of events decreases with E_ν. The pattern of the event number distribution follows the oscillatory picture due to the main $\nu_\mu - \nu_\mu$ mode of the oscillations with a clear distortion in the resonance region. The maxima and minima are approximately along the lines of equal oscillation phases $E_\nu \sim \phi_{32}\Delta m_{32}^2|\cos\theta_z|R_E$ (where R_E is the Earth's radius), again with a distortion in the resonance region $E_\nu = 4 - 10$ GeV. In the high event density bins the numbers of event reach ~ 200, and the total number of events is about $7 \cdot 10^4$.

Introducing the ratios of the fluxes,

$$r \equiv \frac{\Phi_\mu^0}{\Phi_e^0}, \qquad \bar{r} \equiv \frac{\bar{\Phi}_\mu^0}{\bar{\Phi}_e^0},$$

we can rewrite the expression for the density of events (9) as

$$D_\mu^{\mathrm{NH}} = \sigma^{CC}(E_\nu)\Phi_\mu^0\left[\left(P_{\mu\mu} + \frac{1}{r}P_{e\mu}\right) + \kappa_\mu\left(\bar{P}_{\mu\mu} + \frac{1}{\bar{r}}\bar{P}_{e\mu}\right)\right], \tag{11}$$

where

$$\kappa_\mu \equiv \frac{\bar{\sigma}^{CC}\bar{\Phi}_\mu^0}{\sigma^{CC}\Phi_\mu^0}.$$

Recall that the ratio $r \equiv \Phi_\mu^0/\Phi_e^0$ depends both on the neutrino energy and zenith angle, e.g., in the range $E_\nu = (2-25)$ GeV and for $\cos\theta_z = -0.8$ the ratio can be roughly parameterized as $r = 1.2 \cdot (E_\nu/1 \text{ GeV})^{0.65}$.

B. Hierarchy asymmetry

Let us consider the effects of neutrino mass hierarchy on the distribution of the ν_μ events. Using relations (7) we can write the density of the events for the inverted mass hierarchy in terms of the oscillation probabilities for the normal mass hierarchy as

$$D_\mu^{\mathrm{IH}} = \sigma^{CC}\Phi_\mu^0\left[\left(\bar{P}_{\mu\mu} + \frac{1}{r}\bar{P}_{e\mu}\right) + \kappa_\mu\left(P_{\mu\mu} + \frac{1}{\bar{r}}P_{e\mu}\right)\right]. \tag{12}$$

Then the difference of the numbers of events for the inverted and normal mass hierarchies equals

$$N_{ij,\mu}^{\mathrm{IH}} - N_{ij,\mu}^{\mathrm{NH}} = 2\pi N_A\rho T \int_{\Delta_i\cos\theta_z} d\cos\theta_z \int_{\Delta_j E_\nu} dE_\nu V_{\mathrm{eff}}(D_\mu^{\mathrm{IH}} - D_\mu^{\mathrm{NH}}),$$

where

$$D_\mu^{\mathrm{IH}} - D_\mu^{\mathrm{NH}} = \sigma^{CC}\Phi_\mu^0\left[(1-\kappa_\mu)\left(\bar{P}_{\mu\mu} - P_{\mu\mu}\right) + \frac{1}{r}(1-\kappa_e)\left(\bar{P}_{e\mu} - P_{e\mu}\right)\right], \tag{13}$$
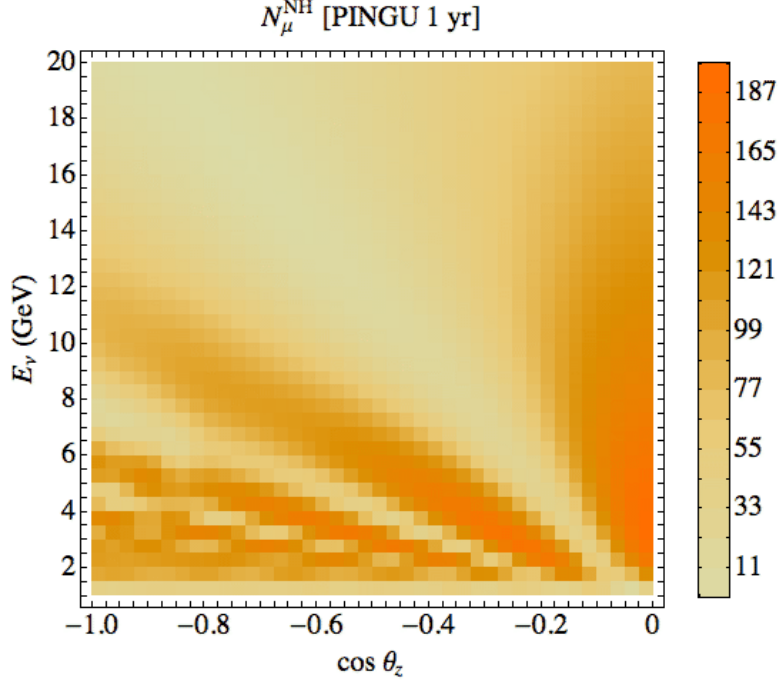
10

FIG. 4: The fine-binned distribution of the number of ν_μ–like events in the $(E_\nu - \cos\theta_z)$ plane that can be collected by the PINGU detector during 1 year; NH is assumed.

and

$$\kappa_e \equiv \frac{\bar{\sigma}^{CC}\bar{\Phi}^0_e}{\sigma^{CC}\Phi^0_e} = \kappa_\mu \frac{r}{\bar{r}} \; .$$

In the approximation $\bar{P}_A \approx 0$, which is justified if the true hierarchy is the normal one, we obtain $\bar{P}_{e\mu} \approx 0$ and

$$\bar{P}_{\mu\mu} \approx 1 - \frac{1}{2}\sin^2 2\theta_{23}\left[1 - \cos\phi_{32}\right],$$

where we have taken $\bar{\phi}_X \approx \phi_{32}$. Consequently,

$$\begin{aligned}
\bar{P}_{\mu\mu} - P_{\mu\mu} &\approx \frac{1}{2}\sin^2 2\theta_{23}\left[\cos\phi_{32} - \sqrt{1 - P_A}\cos\phi_X\right] + s^4_{23}P_A \;, \\
\bar{P}_{e\mu} - P_{e\mu} &\approx -s^2_{23}P_A.
\end{aligned} \quad (14)$$

In this approximation

$$\begin{aligned}
D^{\mathrm{NH}}_\mu &\approx \sigma^{CC}\Phi^0_\mu\left[\left(1 - \frac{1}{2}\sin^2 2\theta_{23}\right)(1 + \kappa_\mu) - s^2_{23}\left(s^2_{23} - \frac{1}{r}\right)P_A + \right. \\
&\left. + \; \frac{1}{2}\sin^2 2\theta_{23}\left(\kappa_\mu\cos\phi_{32} + \sqrt{1 - P_A}\cos\phi_X\right)\right].
\end{aligned}$$

The sensitivity of this quantity to the neutrino mass hierarchy is due to $P_A \neq 0$, and so the highest sensitivity is expected in the kinematic region where P_A is relatively large.

For the difference of the numbers of events for the two hierarchies (13) we obtain

$$D_\mu^{\mathrm{IH}} - D_\mu^{\mathrm{NH}} \approx \sigma^{CC}\Phi_\mu^0 \left\{ \frac{1}{2}\sin^2 2\theta_{23}(1-\kappa_\mu)\left(\cos\phi_{32} - \sqrt{1-P_A}\cos\phi_X\right) + \right.$$
$$\left. + \; s_{23}^2\left[(1-\kappa_\mu)s_{23}^2 - \left(\frac{1}{r} - \frac{\kappa_\mu}{\bar{r}}\right)\right]P_A \right\}.$$

Let us introduce the N-I hierarchy asymmetry for the ij-bin in the $(E_\nu - \cos\theta_z)$ plane as

$$A_{\mu,ij}^{N-I} \equiv \frac{N_{\mu,ij}^{IH} - N_{\mu,ij}^{NH}}{\sqrt{N_{\mu,ij}^{NH}}}. \tag{15}$$

The moduli of the asymmetries (15) are the measure of statistical significance of the difference of the number of events for the normal and inverted mass hierarchies: $S_{ij} = |A_{ij}|$.

Let us consider the condition $N_{ij,\mu}^{\mathrm{IH}} = N_{ij,\mu}^{\mathrm{NH}}$ which gives the borders of the regions in the $(E_\nu - \theta_z)$ plane where the difference of the numbers of events has definite sign. It coincides approximately with the condition $D_\mu^{\mathrm{IH}} = D_\mu^{\mathrm{NH}}$. The latter determines the lines of zero N-I hierarchy asymmetry. Using eq. (13) and approximate expressions in (14) we find from this condition

$$\cos\phi_{32} - \sqrt{1-P_A}\cos\phi_X = \frac{P_A}{2c_{23}^2}\left[\frac{1}{r}\cdot\frac{1-\kappa_e}{1-\kappa_\mu} - s_{23}^2\right]. \tag{16}$$

The phases ϕ_{32} and ϕ_X are functions of E_ν and θ_z. Since $\cos\phi_{32}$ varies with $(\cos\theta_z/E_\nu)$ much faster than $r(E_\nu,\theta_z)$, it is this periodic function that determines the lines of zero hierarchy asymmetry. Our calculations show that eq. (16) determines the zero asymmetry lines rather well.

In Fig. 5 we show the values of the hierarchy asymmetry in the $E_\nu - \cos\theta_z$ plane. The maximal asymmetry is achieved in the low energy parts of the domains bounded by the lines of zero asymmetry (16). The large asymmetry is in the strips along the constant phase lines in the energy interval $E_\nu \approx (4-12)$ GeV, where these lines are distorted by matter effects. The asymmetry changes the sign with changing zenith angle. For instance, in the energy range (7 - 11) GeV there are three distinct zenith angle intervals with the asymmetry sign being the same within each interval. The number of such intervals increases with decreasing energy. Therefore, due to the averaging, the region of high sensitivity to hierarchy will shift to higher energies if the zenith angle reconstruction becomes worse. Furthermore, the regions of high significance of the hierarchy determination overlap substantially with the regions of small numbers of events (see Fig. 4). This means that the significance is enhanced
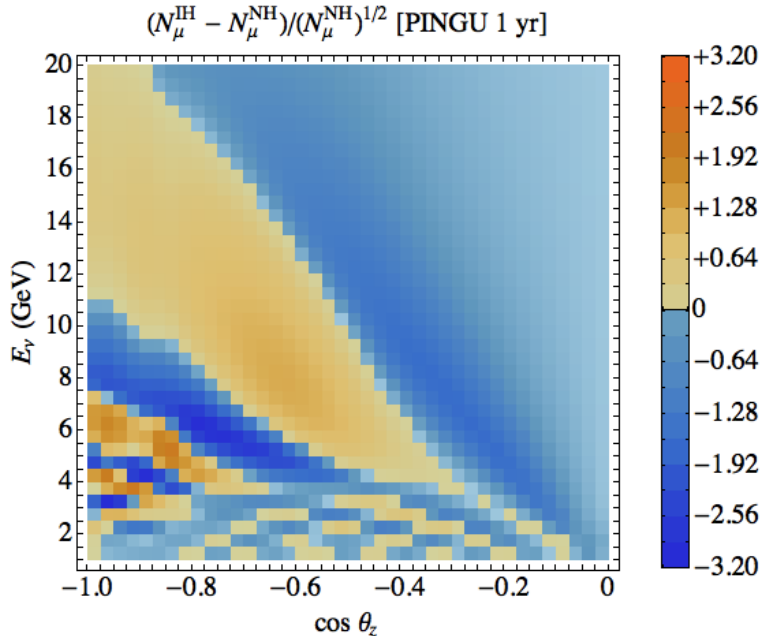
FIG. 5: The hierarchy asymmetry of ν_μ events in the $E_\nu - \cos\theta_z$ plane. The absolute value of the asymmetry in a given bin determines the statistical significance of the difference of the numbers of events for the inverted and normal mass hierarchies.

due to the smallness of the denominator in eq. (15), and it would be diluted by combining a given bin with bins which have higher statistics but smaller significance.

There is an important background to the ν_μ events which comes from ν_τ interactions.

C. ν_τ events

The ν_τ flux appears at the detector due to $\nu_\mu - \nu_\tau$ oscillations. In Fig. 6 we show the distribution of the ν_τ CC events $(\nu_\tau + N \to \tau + X)$ in the $E_\nu - \cos\theta_z$ plane. The figure is a kind of inversion of Fig. 4, with maxima substituted by minima and *vice versa*. The number of events is, however, smaller than the number of ν_μ events due to the smaller cross-section near the threshold. Notice that since ν_τ (as well as ν_l) from the sequential τ decays $(\tau \to \nu_\tau + X, \ \tau \to \nu_\tau + l + \nu_l)$ is not detected, the energy of the original ν_τ cannot be reconstructed.

The ν_τ interactions

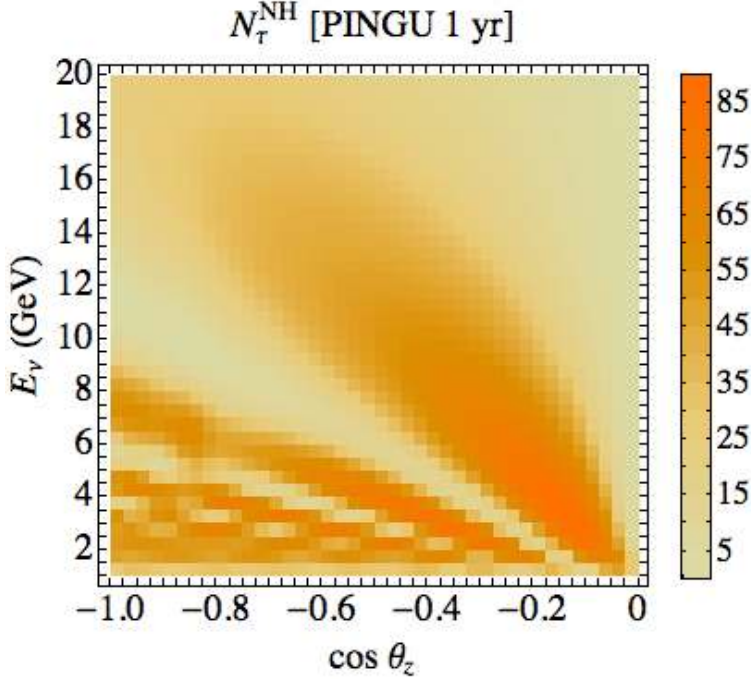$$\nu_\tau + N \to \tau + h \to \mu + \nu + \nu + h \qquad (17)$$

FIG. 6: Same as in Fig. 4, but for ν_τ CC interactions.

will contribute to the main sample of ν_μ events with a muon and a hadronic cascade in the final state. However, the number of these events is relatively small, and in addition these events have certain features which can be used to discriminate them from the true ν_μ events.

Indeed, on average the two neutrinos which appear in the process (17) will take about $1/3$ of the energy of the initial neutrino. Therefore, for a given observed total energy $E_\mu + E_h$, the energy $E_0(\nu_\tau)$ of the original neutrino in the process (17) should be about 1.5 times larger than the energy $E_0(\nu_\mu)$ of the true ν_μ event: $E_0(\nu_\tau)/E_0(\nu_\mu) \approx 1.5$. If only E_μ is used to reconstruct the energy of the original neutrino the rescaling coefficient is $E_0(\nu_\tau)/E_0(\nu_\mu) = 2.5$. On average we can take a factor of 2 for our estimates. Furthermore, the branching ratio of tau decay into muon is $B_\mu = 0.17$. Consequently, the number of ν_μ events due to the reaction chain (17) is suppressed with respect to that of the true CC ν_μ events of the same energy by a factor

$$ B_\mu \left(\frac{E_0(\nu_\tau)}{E_0(\nu_\mu)} \right)^{-1.3} \frac{\sigma_\tau}{\sigma_\mu} \tag{18} $$

(provided that the initial ν_μ and ν_τ fluxes are equal). The power of the second factor follows from the energy dependences of the neutrino flux ($\propto E^{-3}$), the cross-section ($\propto E$) and the effective volume (which we take to be $\propto E^{0.7}$ here; note that in the energy range $E_\nu = 10-35$

14

GeV such a simple power law approximates eq. (10) within 5% error). The last factor takes into account the threshold effect for the τ production. For the energy rescaling factor of 1.5 - 2 we obtain a suppression factor for the number of ν_τ-induced ν_μ events to be $0.05 - 0.08$. Due to the missing energy and momentum taken by the two neutrinos in the final state of reaction (17), the smearing effects in the energy and angle of the original neutrino around the average values will be stronger than for the true ν_μ events. Therefore, the observed energy $E_\mu + E_h$ will have a bigger spread for ν_τ-induced ν_μ events. Furthermore, they will be characterized by a larger average angle between the momenta of the original neutrino and the muon.

There are other properties of reaction (17) which can be utilized to disentangle it from the CC ν_μ detection reaction. In particular, correlations between E_μ and E_h are different for these two cases. Furthermore, one can select $E_\nu - \theta_z$ regions in which the $\nu_\mu - \nu_\tau$ transition probability, and consequently the ν_τ flux, are suppressed. Such regions can be readily found with the help of Fig. 6. The corresponding restriction of the $E_\nu - \theta_z$ parameter space will, of course, result in a loss of the overall statistics, but would provide us with cleaner events. The resulting statistics loss should be affordable because of the extremely high overall statistics in multi-megaton detectors.

In principle, one could also sum up the ν_μ and ν_τ events and consider them in the $\theta_\mu - (E_\mu + E_h)$ plane. However, to determine whether or not a useful information can be extracted from such data would require an additional analysis which is outside the scope of the present paper.

For the above reasons, in what follows we do not explicitly consider the contributions of the $\nu_\tau \to \tau \to \mu$ events and simply treat them as a 5% systematic error.

D. Cascade events and the mass hierarchy

Following the IceCube terminology, we will call the events in which the muon track is not identified as cascade events. There are several different contributions to the cascade events, including even ν_μ events with faint muon tracks which can not be identified. All ν_τ-induced CC events, except those when the tau decays into a muon, contribute to the cascade events.
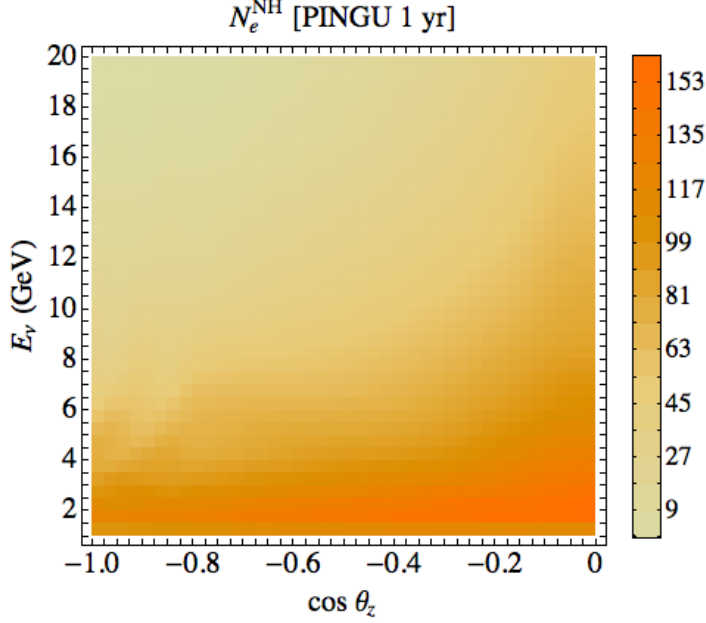
FIG. 7: Same as in Fig. 4 but for ν_e CC interactions; NH is assumed.

For the cascade events $\nu_e + N \rightarrow e + X$ and $\bar{\nu}_e + N \rightarrow e^+ + X$ we have

$$N_{ij,e}^{\mathrm{NH}} = 2\pi N_A \rho T \int_{\Delta_i \cos\theta_z} d\cos\theta_z \int_{\Delta_j E_\nu} dE_\nu V_{\mathrm{eff}}(E_\nu) D_e(E_\nu, \cos\theta_z),$$

where

$$D_e(E, \cos\theta_z) = \sigma^{CC} \Phi_e^0 \left[(P_{ee} + rP_{\mu e}) + \kappa_e \left(\bar{P}_{ee} + \bar{r}\bar{P}_{\mu e} \right) \right].$$

In terms of the probability P_A the number density of events can be written as

$$D_e^{NH} = \sigma^{CC} \Phi_e^0 \left\{ 1 + P_A(rs_{23}^2 - 1) + \kappa_e [1 + \bar{P}_A(\bar{r}s_{23}^2 - 1)] \right\}.$$

The event distribution is shown in Fig. 7. Notice that here the distribution is weakly affected by the oscillations due to a substantial screening effect: the oscillatory part of the number of events contains terms proportional to $rs_{23}^2 - 1$ and $\bar{r}s_{23}^2 - 1$ which are nearly zero at low energies.

The difference of the number densities of events for the inverted and normal mass hierarchies is

$$D_e^{\mathrm{IH}} - D_e^{\mathrm{NH}} = \sigma^{CC} \Phi_e^0 \left(\bar{P}_A - P_A \right) \left[(rs_{23}^2 - 1) - \kappa_e(\bar{r}s_{23}^2 - 1) \right]. \tag{19}$$

The expression in the square brackets here can be rewritten as

$$rs_{23}^2(1 - \kappa_\mu) - (1 - \kappa_e) = (1 - \kappa_\mu) \left[rs_{23}^2 - \frac{1 - \kappa_e}{1 - \kappa_\mu} \right]. \tag{20}$$

16

Thus, there is a double suppression of the difference of numbers of events: (i) due to the neutrino-antineutrino factor $(1 - \kappa_\mu)$ related to the presence of both the neutrino and antineutrino fluxes, and (ii) due to the flavor screening (the last term in eq. (20)) related to the presence of both ν_e and ν_μ in the the original atmospheric neutrino flux [17], more precisely, due to the ratio of these fluxes being close to $1/2$ at low energies. The difference $D_e^{\rm IH} - D_e^{\rm NH}$ can be further suppressed by the smallness of P_A (or of the difference of the neutrino and antineutrino probabilities $\bar{P}_A - P_A$).

The numbers of events for IH and NH are equal, $N_{ij,e}^{\rm IH} = N_{ij,e}^{\rm NH}$, in the bins for which both sides of eq. (20) vanish. From this we obtain

$$s_{23}^2 (r - \bar{r} \kappa_e) = (1 - \kappa_e).$$

For $r \approx \bar{r}$ it gives

$$r(E_\nu, \theta_z) = \frac{1}{s_{23}^2}.$$

So, in this approximation we have only one line of zero asymmetry.

The hierarchy asymmetry in the ν_e CC events is shown in Fig. 8. Maximal asymmetry is in the resonance region $E_\nu = (4 - 8)$ GeV where it has essentially the same sign, so that the suppression due to averaging is absent. Unfortunately, other contributions to the cascade events have different pattern in the $E_\nu - \theta_z$ plane. The number of cascades induced by ν_e quickly decreases with the increase of the neutrino energy.

The dominant contribution to the cascade events comes from the ν_τ flux which appears at the detector due to the oscillations:

$$D_\tau^{NH} = \sigma_\tau^{CC}(E_\nu) \Phi_\mu^0 \left\{ \frac{1}{2} \sin^2 2\theta_{23}[1 - \sqrt{1 - P_A} \cos \phi_X] - c_{23}^2 P_A (s_{23}^2 - 1/r) \right\}.$$

For the ν_τ events the screening due to the flavor composition of the original neutrino flux is absent.

The neutral current interactions of all neutrino species contribute to the total numbers of the cascade events but do not affect the NH-IH differences of events. This reduces the hierarchy asymmetry:

$$A_{cascades} = \frac{N_{e+\tau}^{IH} - N_{e+\tau}^{NH}}{\sqrt{N_{e+\tau}^{NH} + N_{NC}}}.$$

As we will see, analysing only ν_μ events will be sufficient to establish the neutrino mass hierarchy. We therefore do not include cascade events in our discussion. Clearly, cascade
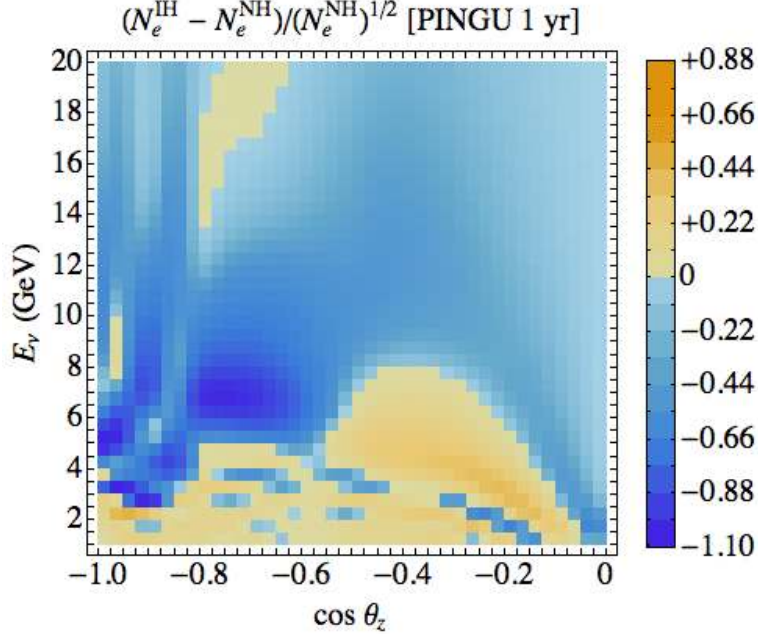
FIG. 8: Same as in Fig. 5 but for ν_e induced events.

events can give additional information, but taking them into account would require a more sophisticated analysis. Notice that possible identification of τ events in a large liquid argon detector and its consequences have been discussed in [22]; should such an identification turn out to be possible also in PINGU, it would increase PINGU's sensitivity to the neutrino parameters.

E. Effects of deviation of the 2-3 mixing from the maximal one

We describe deviation of the 2-3 mixing from the maximal one by

$$d_{23} \equiv \frac{1}{2} - s_{23}^2.$$

From eqs. (11), (2) and (4) we find

$$\begin{aligned}
D_\mu^{NH}(\theta_{23}) - D_\mu^{NH}(\pi/4) &\approx \sigma^{CC}\Phi_\mu^0 \left\{ 2d_{23}^2 \left[1 - \sqrt{1 - P_A} \cos\phi_X \kappa_\mu (1 - \cos\phi_{32}) \right] \right. \\
&+ \left. d_{23}\left(1 - \frac{1}{r} - d_{23}\right) P_A \right\}.
\end{aligned} \tag{21}$$

Notice that both terms in (21) are positive for $\theta_{23} < \pi/4$.

In Fig. 9 we plot statistical significance of the determination of a deviation of the 2-3 mixing from the maximal one. Here again high significance regions coincide with the regions

18

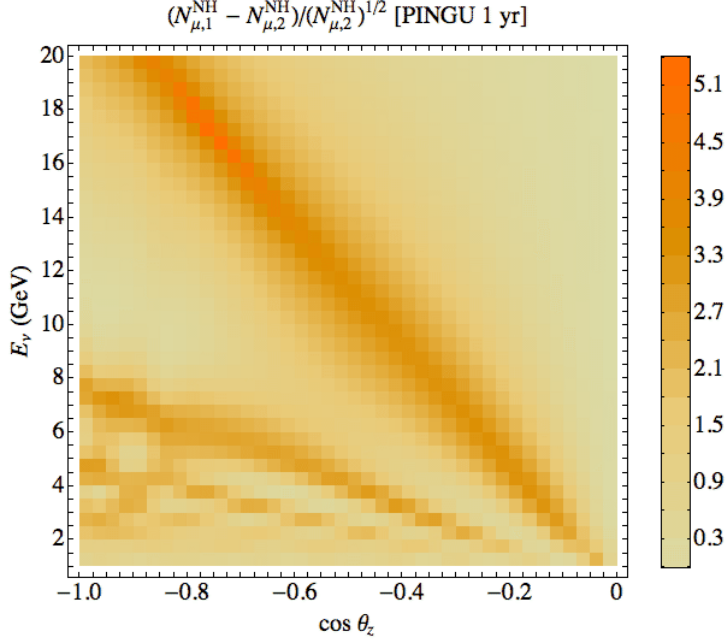$(N_{\mu,1}^{\mathrm{NH}} - N_{\mu,2}^{\mathrm{NH}})/(N_{\mu,2}^{\mathrm{NH}})^{1/2}$ [PINGU 1 yr]

FIG. 9: Statistical significance of the determination of the deviation of the 2-3 mixing from the maximal one. The difference of the tracking events for two values of the 2-3 mixing: $\sin^2 \theta_{23} = 0.5$ $(N_{\mu,1}^{NH})$ and 0.42 $(N_{\mu,2}^{NH})$.

of low density of events (compare Figs. 9 and 4). This means that an integration over large $E_\nu - \cos \theta_z$ domains would lead to a dilution of the significance.

F. CP-violation effects

We can write the oscillation probabilities in the presence of a Dirac-type CP-phase δ as

$$P_{\alpha\beta} = P_{\alpha\beta}^0 + P_{\alpha\beta}^\delta. \tag{22}$$

Here $P_{\alpha\beta}^0$ and $P_{\alpha\beta}^\delta$ are the δ-independent and δ-dependent parts of the oscillation probability $P_{\alpha\beta}$, respectively (note that $P_{\alpha\beta}^0 \neq P_{\alpha\beta}^{\delta=0}$). In a matter with symmetric density profile one has $P_{\beta\alpha} = P_{\alpha\beta}(\delta \to -\delta)$.

Now the 1-2 mass splitting and mixing should be taken into account. The state $\tilde{\nu}_2$ does not decouple and the oscillation probabilities depend on the matrix elements $A_{e\tilde{2}}$, $A_{\tilde{2}\tilde{3}}$ of the evolution matrix A in the propagation basis. Since the amplitude $A_{\tilde{2}\tilde{3}}$ is doubly suppressed (by small $\Delta m_{21}^2/\Delta m_{31}^2$ and s_{13}), the terms that are quadratic in $A_{\tilde{2}\tilde{3}}$ can be neglected. We

have then [15]:

$$P_{ee}^{\delta} = 0,$$

$$P_{e\mu}^{\delta} = \sin 2\theta_{23} |A_{e\tilde{2}} A_{e\tilde{3}}| \cos(\phi + \delta), \tag{23}$$

$$P_{\mu\mu}^{\delta} = -\sin 2\theta_{23} \cos \delta \left\{ |A_{e\tilde{2}} A_{e\tilde{3}}| \cos \phi + \cos 2\theta_{23} \mathrm{Re}[A_{\tilde{2}\tilde{3}}^*(A_{\tilde{3}\tilde{3}} - A_{\tilde{2}\tilde{2}})] \right\}, \tag{24}$$

where $\phi \equiv \arg(A_{e\tilde{2}}^* A_{e\tilde{3}})$. We will also use the notation $|A_{e\tilde{2}}| \equiv \sqrt{P_S}$, $|A_{e\tilde{3}}| \equiv \sqrt{P_A}$ (where P_A now depends also on the parameters of the 1-2 sector).

Note that the last term in the curly brackets in eq. (24) is small if the 2-3 mixing is sufficiently close to the maximal one, and in addition the amplitude $A_{\tilde{2}\tilde{3}}$ is small. We shall therefore use for our estimates the approximation

$$\cos 2\theta_{23} \mathrm{Re}[A_{\tilde{2}\tilde{3}}^*(A_{\tilde{3}\tilde{3}} - A_{\tilde{2}\tilde{2}})] \approx 0. \tag{25}$$

The δ-dependent part of the expression for the number density of the μ-like events is

$$D_{\mu}^{\delta} \equiv \sigma^{CC} \Phi_{\mu}^0 \left[\left(P_{\mu\mu}^{\delta} + \frac{1}{r} P_{e\mu}^{\delta} \right) + \kappa_{\mu} \left(\bar{P}_{\mu\mu}^{\delta} + \frac{1}{\bar{r}} \bar{P}_{e\mu}^{\delta} \right) \right]. \tag{26}$$

Next, we notice that in the case of normal hierarchy one has $\bar{P}_S \approx 0$, $\bar{P}_A \approx 0$, and in the approximation (25) we therefore have $\bar{P}_{e\mu}^{\delta} \approx \bar{P}_{\mu e}^{\delta} \approx 0$, $\bar{P}_{\mu\mu}^{\delta} \approx 0$. From eqs. (23) and (24) we find

$$D_{\mu}^{\delta} - D_{\mu}^{\delta=0} = \sigma^{CC} \Phi_{\mu}^0 \sin 2\theta_{23} \sqrt{P_A P_S} \left[\frac{r-1}{r} \cos \phi (1 - \cos \delta) - \frac{1}{r} \sin \phi \sin \delta \right]. \tag{27}$$

This, in particular, means that the difference $N_{\mu}^{\delta} - N_{\mu}^{\delta=0}$ should nearly vanish whenever $P_S = 0$ or $P_A = 0$, i.e. along the so-called solar and atmospheric "magic" lines [15, 23–25]. The vanishing of the difference $N_{\mu}^{\delta} - N_{\mu}^{\delta=0}$ is, however, not exact, as it relies on the approximation (25). In Figs. 10 - 11 we show statistical significance of measurements of the CP-phase. The strongest effect is at low energies: $E \sim 3 - 5$ GeV. Notice that with increasing δ the size of the asymmetry increases, but the regions of different signs of the asymmetry do not change. This is in agreement with eq. (27). Indeed, in this equation the dependences of the right-hand side on ϕ and δ effectively factorize, because in most of the parameter space either the first or the second term dominates. For the ν_e-like events we obtain similarly

$$D_e^{\delta} \equiv \sigma^{CC} \Phi_e^0 \left[(P_{ee}^{\delta} + r P_{\mu e}^{\delta}) + \kappa_e (\bar{P}_{ee}^{\delta} + \bar{r} \bar{P}_{\mu e}^{\delta}) \right] \approx \sigma^{CC} \Phi_e^0 r \sqrt{P_A P_S} \cos(\phi - \delta). \tag{28}$$
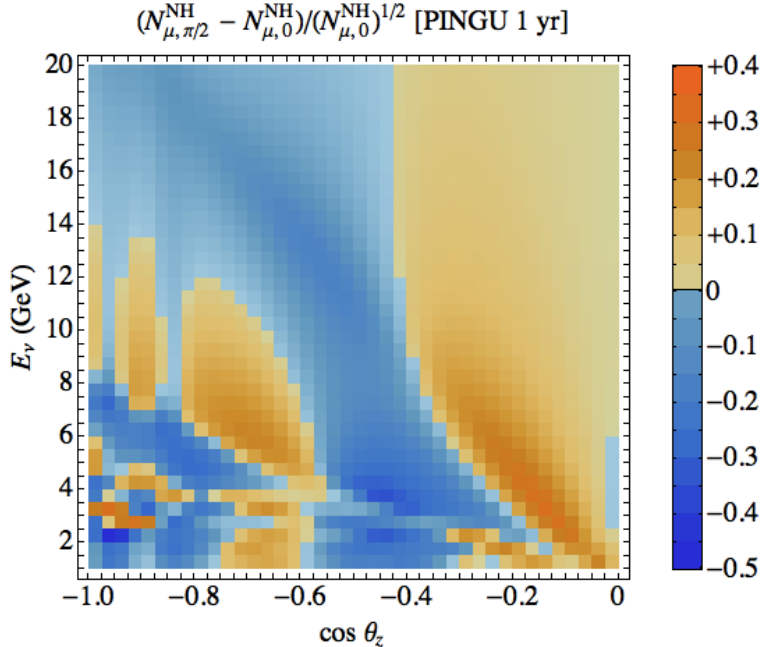
FIG. 10: The difference of the numbers of events for $\delta = \pi/2$ and $\delta = 0$. Statistical significance of measurements of the CP-phase.

Here we have taken into account that P_{ee} and $\bar{P}_{ee}$ are δ-independent and that $\bar{P}_{\mu e}$ is strongly suppressed in matter. For the difference of the densities of ν_e-like events we then find

$$D_e^\delta - D_e^{\delta=0} = \sigma^{CC} \Phi_e^0 r \sin 2\theta_{23} \sqrt{P_A P_S} \left[\cos\phi (\cos\delta - 1) + \sin\phi \sin\delta \right]. \qquad (29)$$

The lines of zero P_A and P_S (the atmospheric and solar "magic" lines) form a grid, which leads to a domain structure in the $(E_\nu - \cos\theta_z)$ plane. For maximal 2-3 mixing the domain structure of the distribution of the events becomes sharper (Fig. 12). As discussed in ref. [15], in the full 3ν framework there is no crossing of the "magic" lines determined by the solar, atmospheric and an additional phase condition, and instead there is a smooth transition of lines of different types into each other.

IV. DETERMINATION OF THE NEUTRINO MASS HIERARCHY

The fine-binned event distributions computed in the previous section allow us to identify the regions of high sensitivity to the neutrino mass hierarchy as well as to other neutrino parameters. They show the lines of zero asymmetry which separate the regions of same sign asymmetry. These distributions also allow one to identify the regions of high and
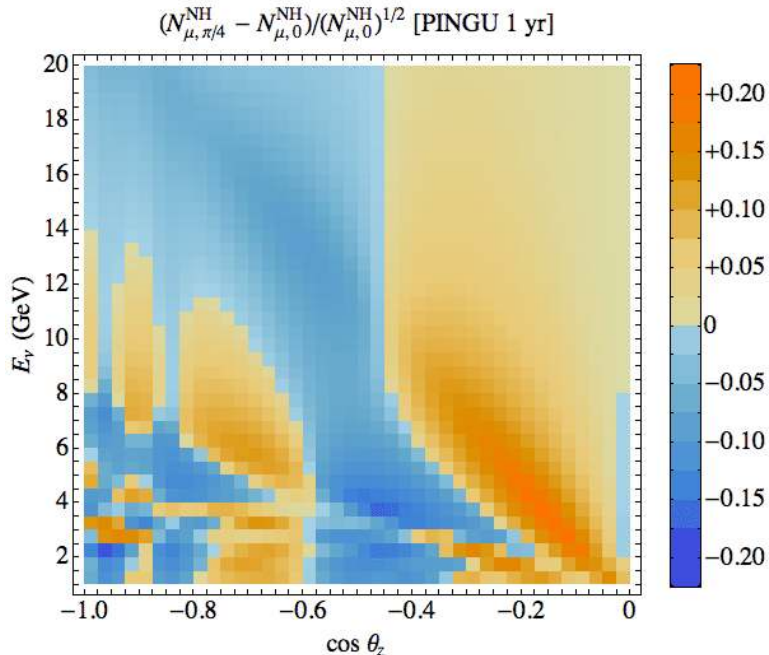
$(N^{\text{NH}}_{\mu,\pi/4} - N^{\text{NH}}_{\mu,0})/(N^{\text{NH}}_{\mu,0})^{1/2}$ [PINGU 1 yr]

FIG. 11: Same as in Fig. 10 but for the phases $\delta = \pi/4$ and $\delta = 0$.

low degeneracy between different parameters. By using them one can select the regions of integration over the neutrino energy and zenith angle in such a way that the hierarchy asymmetry is enhanced while the effects of the uncertainties due to the incomplete knowledge of the other neutrino parameters are canceled or suppressed. Obviously, one should avoid integrating over regions with different signs of the hierarchy asymmetry.

A. Summation of events over different bins

Since one needs to integrate over certain regions of the neutrino energy and zenith angle, the significances of determination of the neutrino mass hierarchy and of other neutrino parameters will be modified in comparison to those found for small individual bins. The combined statistical significance resulting from a summation over n bins is given by

$$S_n = \sum_{i=1}^{n} S_i \sqrt{\frac{N_i^{NH}}{\sum_{k=1}^{n} N_k^{NH}}}.$$

If the individual N_k^{NH} do not differ significantly, we have approximately

$$S_n \approx \frac{1}{\sqrt{n}} \sum_{i=1}^{n} S_i.$$

22

$$\left(N^{\mathrm{NH}}_{\mu,\pi/2} - N^{\mathrm{NH}}_{\mu,0}\right)/\left(N^{\mathrm{NH}}_{\mu,0}\right)^{1/2} \text{ [PINGU 1 yr]}$$
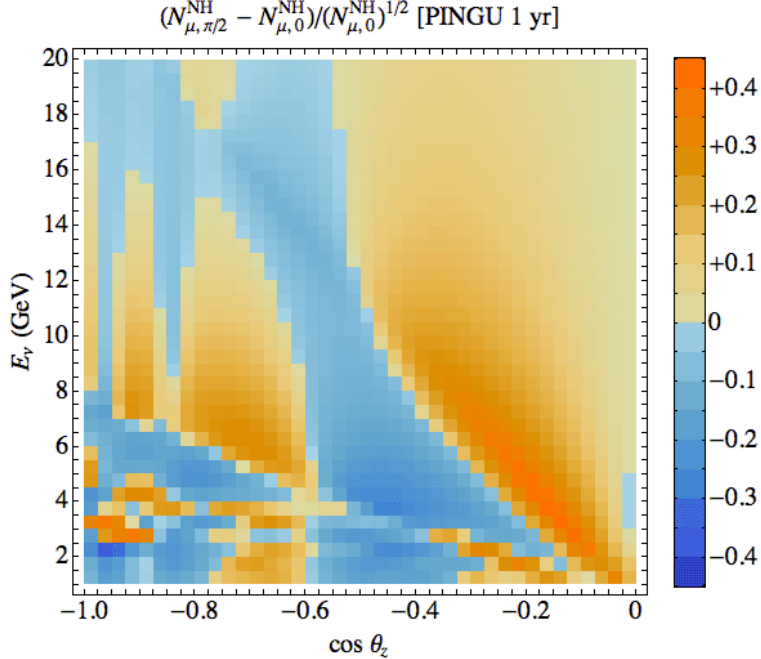
FIG. 12: Same as in Fig. 10 but for phases $\delta = \pi/2$ and $\delta = 0$ and $\sin^2\theta_{23} = 0.5$.

The asymmetry has opposite signs in domains separated by the lines of zero asymmetry, and the ultimate sensitivity to the neutrino mass hierarchy can be estimated as

$$S = \sum_{i=1}^{n} |S_i| \sqrt{\frac{N_i^{NH}}{\sum_{k=1}^{n} N_k^{NH}}} \,.$$

One can first estimate independently the sensitivities of individual domains with the same sign of asymmetry and then sum over the domains. The real sensitivity will actually be lower because of (i) the integration (smearing) over bins with different numbers of events and significances (which will dilute the significance of the most significant bins) (ii) the integration (smearing) over parts of domains which have opposite sign of the asymmetry, (iii) uncertainties of the other oscillation parameters, (iv) degeneracy of parameters, (v) systematic errors, *etc.*. We address some of these issues below.

B. $\nu_\mu-$ like events and the mass hierarchy

The $\nu_\mu-$events produced by the charged current ν_μ interaction are observed as muon tracks accompanied by hadronic cascades. For these events the energy of the muon E_μ and the direction of its trajectory characterized by the angles θ_μ and ϕ_μ as well as the total energy

of the hadron cascade E_h can be measured. Using this information one can reconstruct the neutrino energy:

$$E_\nu^r \approx E_\mu + E_h - m_N \,,$$

where m_N is the nucleon mass. In fact the calorimetric (time integrated) measurement in IceCube provides directly measurement of E_ν.

The reconstruction of the neutrino direction is more complicated. In the first approximation (at sufficiently high energies) one can simply use $\theta_\nu^r \approx \theta_\mu$ with certain spread which depends on the neutrino energy. More precise determination is in principle possible if one uses also the information about the hadron cascades. Knowledge of the energy of the cascade narrows down the uncertainty in the neutrino direction. Further improvement would be possible if one determines the plane in which the muon and the original quark were propagating. In this plane one can introduce the angle between the muon and neutrino trajectories, θ_ν, as well as the angle between the directions of the quark and neutrino momenta θ_q. Then, using the energy and momentum conservation laws and excluding θ_q, one obtains the expression for the reconstructed neutrino angle:

$$\cos\theta_\nu^r \approx \frac{E_\nu^{r2} + E_\mu^2 - E_h^2}{2E_\nu^r E_\mu} \,,$$

where we assume that the muons are ultra-relativistic. In turn, the knowledge of θ_ν and of the muon angles θ_μ and ϕ_μ would allow one to reconstruct the neutrino zenith angle θ_z^r: $\theta_z^r = \theta_z^r(\theta_\nu, \theta_\mu, \phi_\mu)$.

There is a number of uncertainties in this reconstruction procedure: (i) Errors in the measurements of E_μ, θ_μ and ϕ_μ; (ii) the uncertainty in the point of the neutrino interaction (i.e. of the beginning of the muon trajectory); (iii) the uncertainty in the position of the center of the hadronic shower and (iv) the error in the determination of the energy of the hadron shower.

We will describe the uncertainties of reconstruction of the neutrino parameters by distribution functions for the reconstructed neutrino energies and zenith angles:

$$G_E(E_\nu^r, E_\nu), \quad G_\theta(\theta_z^r, \theta_z),$$

where E_ν and θ_z are the true energy and zenith angle of the neutrinos. The distributions are normalized in such a way that

$$\int dy \, G_y(y^r, y) = 1 \,, \quad y = E_\nu, \theta_z \,,$$

where the integrations are performed within the appropriate ranges of the parameters. For G_y we adopt the Gaussian form

$$G_y(y, \sigma_y) = \frac{N_y}{\sqrt{2\pi}\sigma_y} e^{-\frac{y^2}{2\sigma_y^2}}$$

where N_y is the normalization constant, and σ_E and σ_θ are the widths of the energy and angular reconstruction functions, respectively. Both widths depend on the neutrino energy. In this way we obtain the unbinned distribution of events in the $(E_\nu^r - \cos\theta_z^r)$ plane:

$$D_\alpha(E^r, \cos\theta^r) = \int d\cos\theta_z \int dE_\nu \; G_E(E_\nu^r, E_\nu) \; G_\theta(\theta_z^r, \theta_z) \; V_{\text{eff}} \; N_\alpha(E_\nu, \cos\theta_z), \qquad (30)$$

$\alpha = e, \mu$. Then the binned distributions of events are

$$N_{ij,\alpha}^{\text{NH}} = 2\pi N_A T \rho \int_{\Delta_i(\cos\theta_z^r)} d\cos\theta_z^r \int_{\Delta_j(E_\nu^r)} dE_\nu^r \; D_\alpha(E^r, \cos\theta_z^r). \qquad (31)$$

We will explore the dependence of our results on the widths σ_E and σ_θ. For the ideal resolution, $G_y(y^r, y) = \delta(y^r - y)$, we get from (30) and (31) the same results as before.

Consider the opposite limit of large widths, $2\sigma_y \gg \Delta y$. In this case it is worthwhile to interchange the integrations $dE_\nu^r d\cos\theta_z^r$ and $dE_\nu d\cos\theta_z$. Then for the box-like distribution functions, $G_y = 1/2\sigma_y$ in the intervals $y = y^r \pm \sigma_y$, formulas (30) and (31) reproduce the results for large bins $\Delta y \sim 2\sigma_y$.

For a contained ν_μ event (both the vertex and μ track are contained within the detector) the error in the reconstructed neutrino energy scales linearly with energy, i.e. $\sigma_{E_\nu} \sim x E_\nu$ below ~ 100 GeV [28]. The error in reconstructing the neutrino arrival direction at low energies is limited from below by the root mean square value of the scattering angle, $\theta_{RMS} \sim \sqrt{m_p/E_\nu}$, which corresponds to 17.5° at 10 GeV.

In Figs. 13 - 16 we show the hierarchy asymmetry in the distributions of the ν_μ events smeared with energy-dependent Gaussian reconstruction functions characterized by different σ_E and σ_θ. After smearing we integrated the event density over the reconstructed energy and zenith angle bins of the size $\Delta(E_\nu^r) = 1$ GeV and $\Delta(\cos\theta_z^r) = 0.05$. The smearing leads to a substantial decrease of the sensitivity to the neutrino mass hierarchy. This reduction is a consequence of the integration over regions with different significance and statistics as well as over the regions with different signs of the asymmetry.

Considering the effect in each bin as an independent measurement, we can find the

combined significance as

$$S^{tot} = \sqrt{\sum_{ij} S_{ij}^2} = \sqrt{\sum_{ij} \frac{(N_{ij}^{IH} - N_{ij}^{NH})^2}{\sigma_{ij}^2}},$$

where the sum over bins can be substituted by the integral. For illustration we assume that the uncorrelated systematic errors are proportional to the number of events: $\sigma_{corr} = f N_{ij}^{NH}$, where f depends on the binning. We will use $f = 5\%$ and 10%. In general f is a function of neutrino energy and zenith angle. Therefore the total error in each bin is given by

$$\sigma_{ij}^2 = N_{ij}^{NH} + (f N_{ij}^{NH})^2.$$

Notice that since here the contribution from the systematic error is proportional to N^2, for the same f the role of systematic error decreases with decreasing size of the bin.

Correlated systematic errors, e.g., those of the overall flux normalization and of the tilt of the spectrum, apparently can not reproduce the profile of the distribution of events similar to the difference of distributions for the two hierarchies. Therefore, their effect to a large extent can be reduced to a reduction of the exposure time and statistics. Moreover, these correlated systematic errors can be parameterized and reduced with better measurements of the flux.

Instead of θ_ν, one could consider the angle θ_μ which is measured directly. Smearing over the angle θ_ν with $\sigma_\theta \sim \sqrt{m_p/E_\nu}$ essentially corresponds to the transition from θ_ν to θ_μ. Again, due to measurements of the cascade energy this uncertainty will be further reduced. In Fig. 13 we used $\sigma_E = 0.2 E_\nu$ and $\sigma_\theta = \sqrt{m_p/E_\nu}$. It can be seen from the figure that the region of the highest significance is between the lines $E_\nu/\text{GeV} \approx 20(|\cos\theta_z| - 0.2)$ and $E_\nu/\text{GeV} \approx 15(|\cos\theta_z| - 0.2)$, and between $\cos\theta_z = -1$ to -0.7. It is shifted towards higher energies compared to the un-smeared case in Fig. 5.

Detection of hadronic cascades can in principle improve the determination of the neutrino angle. In Fig. 14 we therefore use the angular resolution $\sigma_\theta = 0.5\sqrt{m_p/E_\nu}$. Notice that with better angular resolution the region of high sensitivity shifts to lower energy and shallower zenith angle bins, approximately along the lines of high significnace.

To study the effect of the energy dependence of σ_E on the neutrino mass hierarchy determination, in Fig. 15 we use the fixed energy resolution $\sigma_E = 2$ GeV and the angular resolution $\sigma_\theta = \sqrt{m_p/E_\nu}$. A comparison with Fig. 13 shows that fixed σ_E leads to a somewhat higher significance of the hierarchy determination.
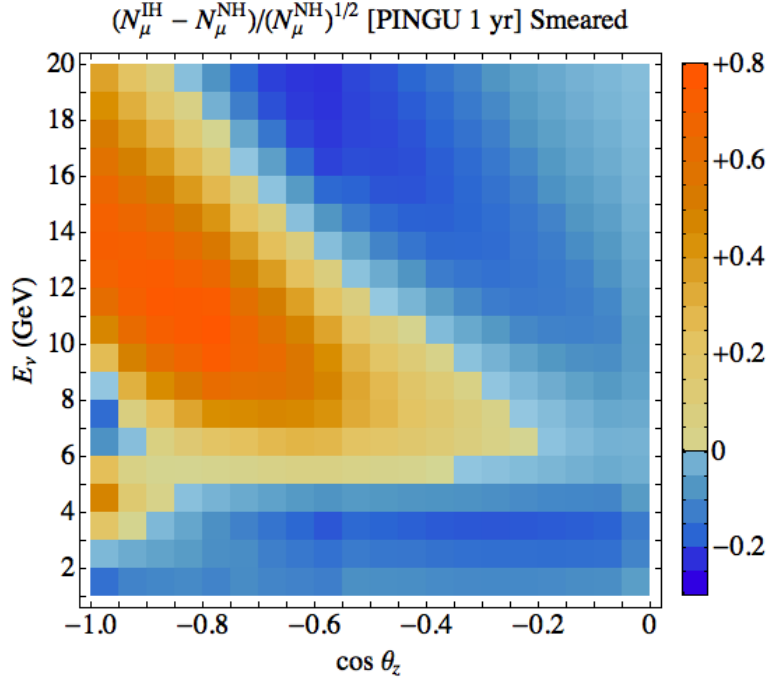
FIG. 13: Statistical significance of the determination of the mass hierarchy after smearing the ν_μ events in the $(E_\nu^r$–$\cos\theta^r)$ plane with $\sigma_E = 0.2 E_\nu$ and $\sigma_\theta = \sqrt{m_p/E_\nu}$.
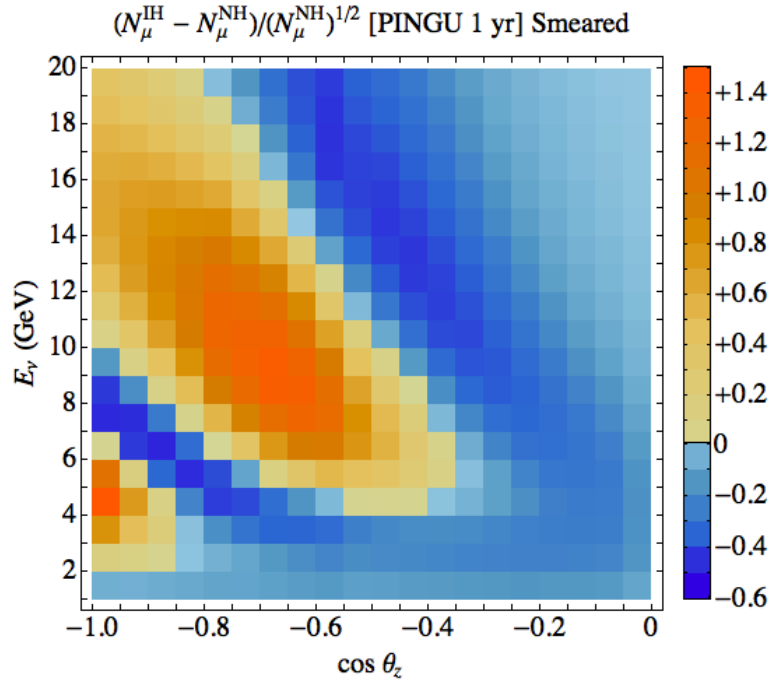

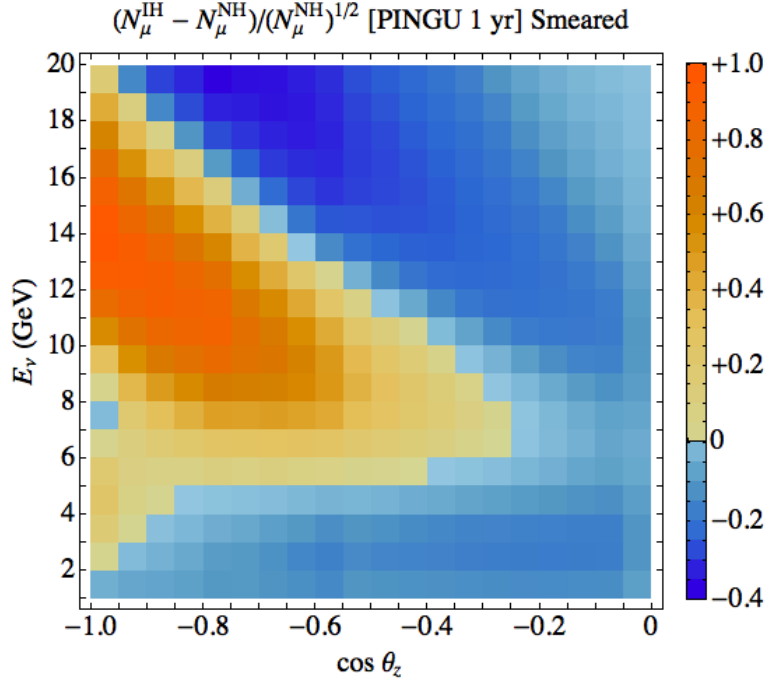FIG. 14: Same as Fig. 13 but for $\sigma_\theta = 0.5\sqrt{m_p/E_\nu}$.

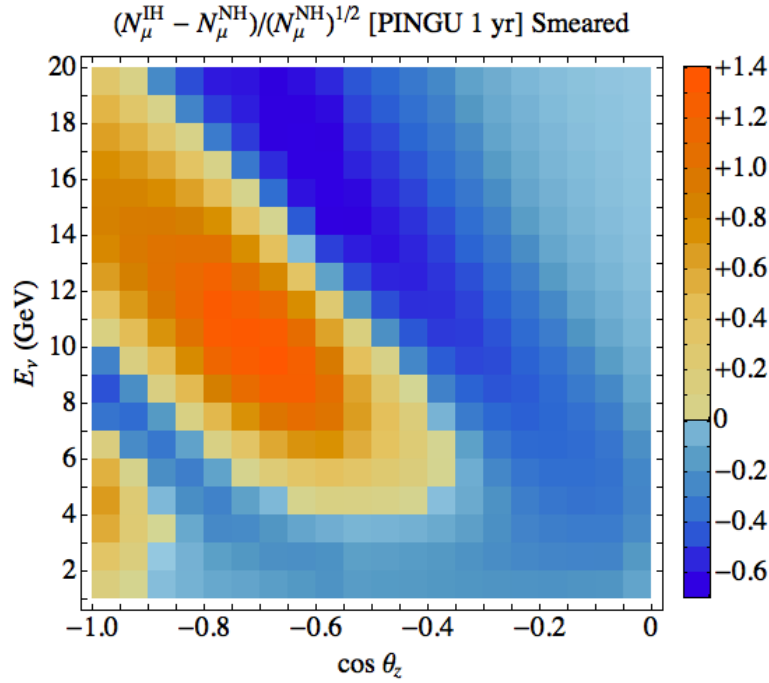FIG. 15: Same as Fig. 13 but for $\sigma_E = 2$ GeV.

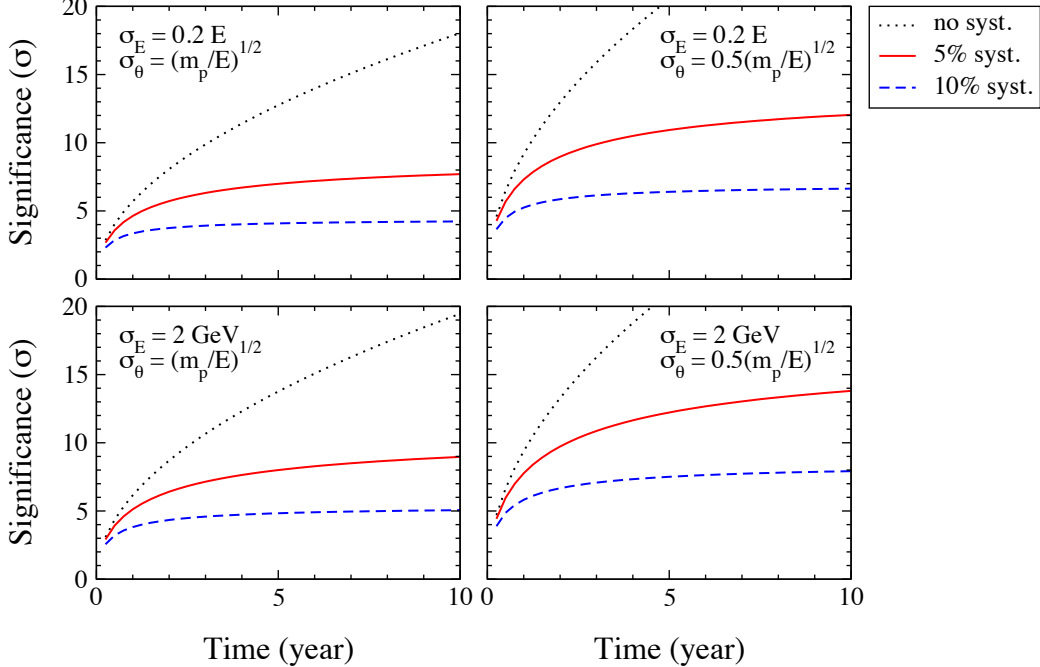FIG. 16: Same as Fig. 13 but with $\sigma_E = 2$ GeV and $\sigma_\theta = 0.5\sqrt{m_p/E_\nu}$.

FIG. 17: Significance of hierarchy determination vs. exposure time for various smearing schemes illustrated in Figs. 13, 14, 15 and 16. Different curves correspond to different systematic uncertainties (f) assumed in addition to statistical uncertainties.

In Fig. 16 we used the energy resolution $\sigma_E = 2$ GeV but the angular resolution $\sigma_\theta = 0.5\sqrt{m_p/E_\nu}$. Figs. 16 and 14 show that with improving angular resolution the significance of the neutrino mass hierarchy determination increases significantly.

Figure 17 shows the significances of the hierarchy identification, S^{tot}, for different smearing schemes described above and for different uncorrelated systematics (f). The 5-year significances from the plots can be compared with the results found when no smearing is performed: $S^{tot} = 45.5\sigma$ (no systematics), $S^{tot} = 28.9\sigma$ ($f = 5\%$) and $S^{tot} = 18.8\sigma$ ($f = 10\%$). Note that if IH is the true hierarchy, then in the first approximation the results simply correspond to Figs. 13 – 16 with reversed signs of the asymmetry, although significances become somewhat lower in general.

C. Effects of parameter degeneracy

In our computations of the hierarchy asymmetry we used the fixed values of Δm_{32}^2, θ_{13}, θ_{23} and δ. In certain kinematic regions, uncertainties in these parameters may lead to the
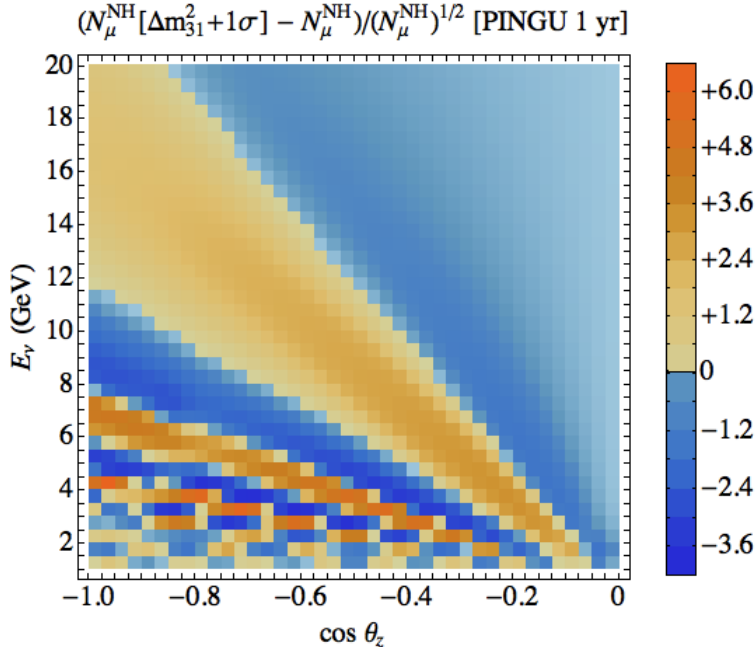
FIG. 18: Effect of uncertainty in Δm_{31}^2. Shown is the difference of numbers of events for Δm_{31}^2 and $\Delta m_{31}^2 + 1\sigma = 2.47 \cdot 10^{-3}$ eV^2. NH is assumed.

same effects as the hierarchy change. That is, the difference of the event distributions for the true and assumed values of the parameters may have the same pattern as the difference of event distributions for the normal and inverted mass hierarchies. The simplest way to reduce the degeneracy is to select only parts of the $E_\nu - \cos\theta_z$ space where the effect of hierarchy change dominates over other effects.

1. As follows from the comparison of Figs. 10, 11, 12 and Fig. 5, the effect of CP-phase δ at high energies is smaller than 10% of the hierarchy effect, and so it can be neglected in the first approximation. Also, it is characterized by a different pattern, and therefore one can select the regions in the $E_\nu - \cos\theta_z$ plane in such a way as to further suppress the effect of the CP-phase (e.g. the selected bins should include domains with different signs of CP-asymmetry). We computed the hierarchy asymmetry for $\delta = \pi/2$ and found that indeed the CP effect can be neglected in the first approximation.

2. Effects of the uncertainty in θ_{23} are strong in the region along the line $E_\nu/\text{GeV} \approx 23|\cos\theta_z|$ (Fig. 9). In the high energy part of this region, $E > 10$ GeV, the hierarchy asymmetry is small. There is still an overlap of the regions of large effects of the hierarchy and θ_{23} uncertainty at low energies. The bins can be selected in such a way that the

effect of the uncertainty in θ_{23} substantially cancels out. Furthermore, one expects some improvements in the determination of θ_{23} from the accelerator and combination of reactor and accelerator experiments, so that the degeneracy will be further reduced. In particular, combining the reactor data with the forthcoming results from T2K and NOvA will allow us to determine $\sin^2\theta_{23}$ with an accuracy between about 0.04 (for maximal 2-3 mixing) and 0.008 (for $\sin^2\theta_{23} = 0.4$) [26]. This has to be compared with the current uncertainty of this parameter $\delta(\sin^2\theta_{23}) \simeq 0.05$ [27] (all numbers correspond to 1σ).

3. The effect of uncertainty in Δm_{31}^2 is illustrated in Fig. 18, where we show the difference of numbers of events for the best fit and shifted upwards by 1σ values of Δm_{31}^2. (A downward shift by 1σ switches signs in Fig. 18, although with somewhat smaller significances.) In the limit $\Delta m_{21}^2 = 0$ variations of Δm_{31}^2 are equivalent to a corresponding shift of the oscillatory pattern in the energy scale (see Fig. 2) at high energies ($E > 8$ GeV). Note that the shift is different for different zenith angles and for neutrinos and antineutrinos. The regions of the strongest effect of this shift on the hierarchy asymmetry have substantial overlap with the regions of strong hierarchy asymmetry, and therefore certain selection of the integration regions (binning) is required in order to reduce the degeneracy and disentangle the two effects. Clearly, further improvements of the accuracy of measurements of Δm_{31}^2 by MINOS, T2K and NOvA will alleviate this problem. In particular, T2K and NOvA will measure Δm_{31}^2 with an accuracy of 5×10^{-5} eV^2 (1σ) [26]. This is about a factor of two better than the current uncertainty of this parameter [27].

To further explore if the uncertainty in Δm_{31}^2 can mimic the "wrong" hierarchy, we applied the same $\sigma_E = 0.2 E_\nu$ and $\sigma_\theta = \sqrt{m_p/E_\nu}$ smearing as in Fig. 13 to the best-fit and $+1\sigma$ deviation of the Δm_{31}^2 values. The resulting significances are plotted in Fig. 19. Note that the region of the highest sensitivity to Δm_{31}^2 has shifted to higher energies and is concentrated in a narrower, $\cos\theta_z < -0.8$, range as compared to the region of the highest significance of the hierarchy asymmetry (cf. Figs. 19 and 13).

Figure 20 shows the difference between the significances plotted in Figs. 19 and 13. Notice that the significances of the hierarchy determination in the region $E_\nu \simeq 6 - 13$ GeV are reduced considerably. The effect of the degeneracy can be suppressed by making summation of significances only over certain domains in the $E_\nu - \cos\theta_z$ plane.

To estimate the effect of the uncertainty of the value of Δm_{31}^2 on the significance of the hierarchy determination, we simulated the data for NH N_μ^{NH} for a fixed "true" value
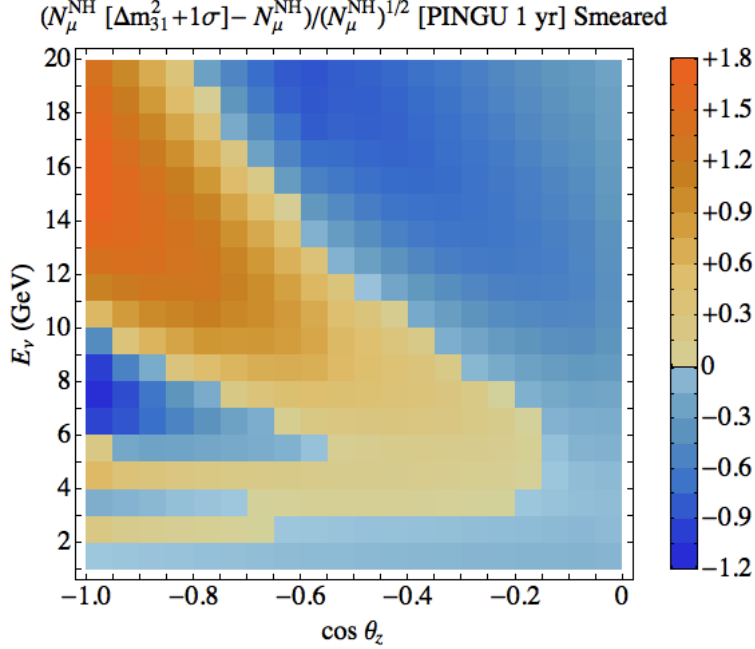
FIG. 19: Same as in Fig. 18 but after smearing the ν_μ events in the $(E^r_\nu$–$\cos\theta^r)$ plane with $\sigma_E = 0.2E_\nu$ and $\sigma_\theta = \sqrt{m_p/E_\nu}$.

of $\Delta m^2_{31,true}$ and then fitted them with IH, treating Δm^2_{23} as a free parameter. We then minimized S^{tot} with respect to Δm^2_{32} and found the corresponding values of $\Delta m^2_{23,fit}$ and S^{tot}_{min}. Next, we repeated the same procedure for different true values of $\Delta m^2_{31,true}$ within its 1σ allowed range. This procedure is illustrated in Fig. 21. The left panel shows S^{tot} versus $\Delta m^2_{32,fit}$ for $\Delta m^2_{31,true} = 2.35 \cdot 10^{-3}$ eV^2 (vertical line). In the right panel of Fig. 21 we show the values of S^{tot}_{min} obtained through this procedure as functions of $\Delta m^2_{31,true}$ (solid lines). For comparison we show also S^{tot} for $\Delta m^2_{23,fit} = \Delta m^2_{31,true}$, i.e. without variations of $\Delta m^2_{23,fit}$ (dashed lines). As follows from the figure, variation of $\Delta m^2_{23,fit}$ reduces the significance of the hierarchy identification S^{tot} by $\sim 50\%$, and this reduction weakly depends on $\Delta m^2_{31,true}$. The values $\Delta m^2_{23,fit,min}$ are within the present 2σ uncertainties of determination of this mass difference $(2.17 \cdot 10^{-3} - 2.59 \cdot 10^{-3})$ eV^2 [18]. To calculate the significances presented in the figure we have smeared the event distributions with $\sigma_E = 0.2E_\nu$ and $\sigma_\theta = \sqrt{m_p/E_\nu}$ as in Fig. 13.
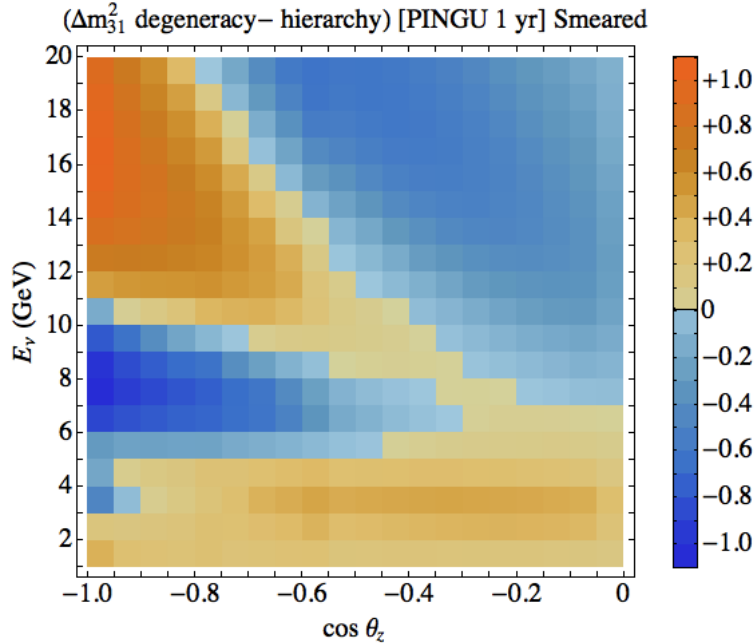
FIG. 20: Difference of significances in the (E_ν^r–$\cos\theta^r$) plane between the Δm_{31}^2 uncertainty (Fig. 19) and the mass hierarchy (Fig. 13).

V. CONCLUSIONS

The main goal of our paper was to attract attention to the possibility of determination of the neutrino mass hierarchy with huge atmospheric neutrino detectors like PINGU, to propose a method of quick estimation of the sensitivity of such detectors to the mass hierarchy and to outline challenges on the way of realization of this idea.

1. After the determination of the leptonic 1-3 mixing angle, the structure of the neutrino oscillograms discussed in refs. [14] and [15] (see also Fig. 3) is well determined, and the position of the main structures in the $E_\nu - \cos\theta_z$ (kinematic) plane is fixed. For $E_\nu > 1$ GeV these include the MSW resonance in the Earth's mantle domain as well as the MSW resonance and the three parametric ridges in the core domain of the oscillograms.

2. The multi-megaton ice (water) detectors like PINGU will allow one to reconstruct the oscillograms and determine yet unknown neutrino parameters: the mass hierarchy (the sign of Δm_{31}^2), the deviation of the 2-3 mixing from the maximal one, and in principle, the CP-violation phase as the next step. In addition, once the neutrino mass hierarchy has been established, the data from multi-megaton detectors should allow a significantly better
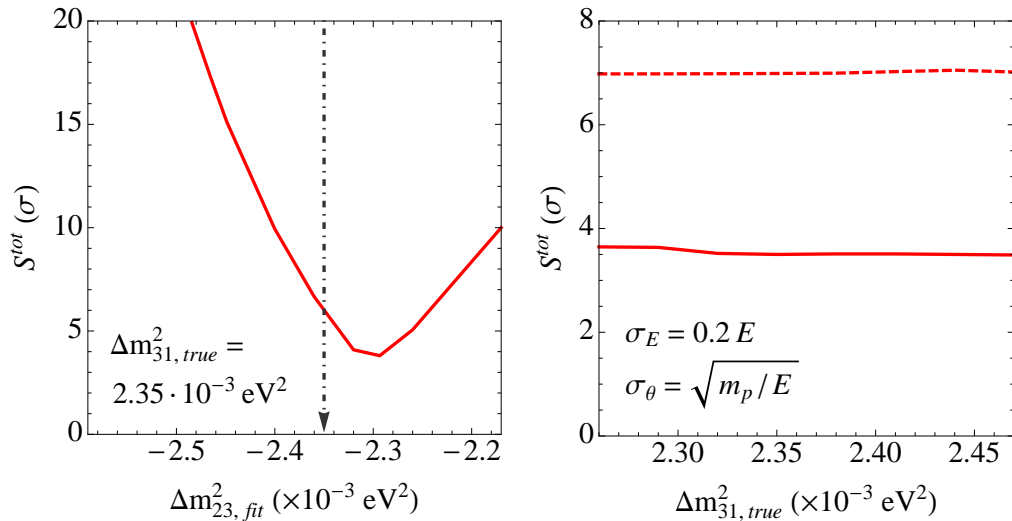
FIG. 21: *Left panel*– Significance of determination of the hierarchy as a function of the "fit" values of $\Delta m^2_{23,fit}$ when the "true" value of $\Delta m^2_{31,true} = 2.35 \cdot 10^{-3}$ eV^2 (vertical line). *Right panel* – Significances as functions of $\Delta m^2_{31,true}$ after minimization as in the left panel (solid lines) and when $\Delta m^2_{23,fit} = \Delta m^2_{31,true}$ (dashed lines). A systematic uncertainty $f = 5\%$ and 5-yr PINGU data was used.

determination of the value of Δm^2_{31}.

3. At the probability level the effects of the change of the mass hierarchy and of variations of θ_{23} can be of order 1. However, there are several factors that substantially reduce the effects at the level of observable events. We have identified and studied in detail the following factors:

a) $\nu - \bar{\nu}$ summation, which is related to the presence of both neutrinos and antineutrinos in the original neutrino flux. The hierarchy asymmetry survives due to a factor of ~ 2 difference of the neutrino and antineutrino cross-sections as well as some difference of the original neutrino fluxes.

b) Flavor screening, which leads to the suppression factors like $(s^2_{23}r - 1)$ and $(s^2_{23}\bar{r} - 1)$ and is related to the presence of both ν_e and ν_μ in the original flux.

c) Dilution of the significance: often large significances of the hierarchy asymmetry and other event number differences appear in bins where numbers of events are small. Then summation of signals in these high-significance bins and in bins where the numbers of events are larger but the significance is lower leads to a dilution of the high significance.

d) Smearing: finite energy and angular resolutions mean that integrations over rather large domains in the $E_\nu - \theta_z$ plane have to be performed. These domains usually contain regions with different signs of the considered effect (e.g., hierarchy asymmetry). Therefore the integration leads to a significant suppression of the studied effects.

e) Parameter degeneracies.

4. We presented the significance plots for the determination of the neutrino mass hierarchy, deviation of the 2-3 mixing from the maximal one and CP-phase.

5. To evaluate the possibility to establish the neutrino mass hierarchy, we performed smearing of the event number distributions using Gaussian functions for reconstructing the true neutrino energies and zenith angles. We have studied the dependence of the significances integrated over certain ranges of E_ν and $\cos\theta_z$ on the widths of the reconstruction functions. Our preliminary estimates show that after 5 years of PINGU 20 operation the significance of the determination of the hierarchy can range from $\sim 3\sigma$ to 10σ (with parameter degeneracies taken into account), depending on the accuracy of reconstruction of the neutrino energy and zenith angle.

6. The smearing procedure implemented in this paper captures the main uncertainties of reconstruction of the true neutrino energies and zenith angles rather accurately. The smearing we have adopted gives a good estimate (at least at this stage of knowledge of future experimental characteristics) of the accuracy of reconstruction of the neutrino parameters. By varying the smearing parameters in rather wide ranges we covered essentially all possibilities of practical interest and explored the detecor resolutions necessary to achieve a given significance of the hierarchy determination.

7. The parameter degeneracy effects can be significant, so that similar patterns of event distribution in the $E_\nu - \theta_z$ plane or in its parts can be obtained due to either changing the neutrino mass hierarchy or due to variations of the 2-3 mixing or of Δm_{31}^2 within their currently allowed ranges. For each parameter we identified the kinematic regions of the smallest degeneracy (where the effect we are interested in dominates). The effects of the parameter degeneracy can be reduced by selecting particular regions of integration over E_ν and $\cos\theta_z$. In addition, forthcoming measurements of neutrino parameters (in MINOS, T2K, NOvA and in reactor experiments) should provide us with more accurate values of these parameters and further reduce the effects of parameter degeneracy.

Acknowledgments

Appendix. Proof of the relation $\bar{P}_{\alpha\beta} = P_{\alpha\beta}(\Delta \to -\Delta)$ in the limit $\Delta m_{21}^2 \to 0$

Let us prove that in the limit $\Delta m_{21}^2 \to 0$ the oscillation probabilities for antineutrinos are given by those for neutrinos with the substitution $\Delta m_{31}^2 \to -\Delta m_{31}^2$. A slightly different proof of this statement can be found in [29].

The evolution equation for the neutrino state vector in the propagation basis is

$$i\frac{d}{dx}\tilde{\nu} = \tilde{H}(x)\tilde{\nu}\,, \tag{32}$$

where $\tilde{\nu} = (\nu_e, \nu_{\tilde{2}}, \nu_{\tilde{3}})$ and the effective Hamiltonian $\tilde{H}(x)$ in the limit $\Delta m_{21}^2 \to 0$ takes the form

$$\tilde{H}(x) = \begin{pmatrix} s_{13}^2\Delta + V(x) & 0 & s_{13}c_{13}\Delta \\ 0 & 0 & 0 \\ s_{13}c_{13}\Delta & 0 & c_{13}^2\Delta \end{pmatrix}. \tag{33}$$

Here $\Delta \equiv \Delta m_{31}^2/2E$. The evolution matrix (the matrix of the transition amplitudes) then has the form

$$A(x) = \begin{pmatrix} A_{ee} & 0 & A_{e\tilde{3}} \\ 0 & 1 & 0 \\ A_{\tilde{3}e} & 0 & A_{\tilde{3}\tilde{3}} \end{pmatrix} \tag{34}$$

From unitarity of this matrix it follows that $|A_{\tilde{3}e}| = |A_{e\tilde{3}}|$. For antineutrinos, one has to flip the sign of the potential $V(x)$ in eq. (33). Obviously, this is equivalent to flipping the sign

of Δ in (33) and additionally changing the overall sign of the Hamiltonian $\tilde{H}(x)$. The latter can be compensated by complex conjugating the evolution equation (32). Thus, we find

$$A(\bar{\nu}, \Delta) = A^*(\nu, -\Delta).$$

(35)

Recall now that in the limit $\Delta m_{21}^2 \to 0$ the probabilities of various flavour transitions are expressed only through $P_A = |A_{e\tilde{3}}|^2$ and $\cos \phi_X$ where $\phi_X = arg(A_{\tilde{2}\tilde{2}} A_{\tilde{3}\tilde{3}}^*) = arg(A_{\tilde{3}\tilde{3}}^*)$ (see eqs. (1)-(5)). Therefore we find that the oscillation probabilities for antineutrinos are given by those for neutrinos of the opposite neutrino mass hierarchy (*i.e.* with $\Delta \to -\Delta$).

---

[1] L. Wolfenstein, Phys. Rev. D **17** (1978) 2369.

[2] S. P. Mikheev and A. Y. Smirnov, Sov. J. Nucl. Phys. **42** (1985) 913 [Yad. Fiz. **42** (1985) 1441].

[3] V. K. Ermilova, V. A. Tsarev and V. A. Chechin, Kr. Soob, Fiz. [Short Notices of the Lebedev Institute] **5** (1986) 26; E. K. Akhmedov, Sov. J. Nucl. Phys. **47** (1988) 301 [Yad. Fiz. **47** (1988) 475]; preprint IAE-4470/1, 1987.

[4] Y. Fukuda *et al.* [Super-Kamiokande Collaboration], Phys. Rev. Lett. **81** (1998) 1562 [hep-ex/9807003].

[5] T. Kajita, Nucl. Phys. Proc. Suppl. **217** (2011) 157.

[6] M. C. Gonzalez-Garcia and M. Maltoni, Phys. Rev. D **70** (2004) 033010 [hep-ph/0404085].

[7] J. Bernabeu, S. Palomares Ruiz and S. T. Petcov, Nucl. Phys. B **669** (2003) 255 [hep-ph/0305152]; D. Indumathi and M. V. N. Murthy, Phys. Rev. D **71** (2005) 013001 [hep-ph/0407336]; M. C. Gonzalez-Garcia, M. Maltoni and A. Y. Smirnov, Phys. Rev. D **70** (2004) 093005 [hep-ph/0408170]; R. Gandhi, P. Ghoshal, S. Goswami, P. Mehta and S. U. Sankar, Phys. Rev. D **73** (2006) 053001 [hep-ph/0411252]; S. T. Petcov and T. Schwetz, Nucl. Phys. B **740** (2006) 1 [hep-ph/0511277]; R. Gandhi, P. Ghoshal, S. Goswami and S. U. Sankar, Phys. Rev. D **78** (2008) 073001 [arXiv:0807.2759 [hep-ph]]; T. Schwetz, Nucl. Phys. Proc. Suppl. **188** (2009) 158 [arXiv:0812.2392 [hep-ph]]; A. Samanta, Phys. Rev. D **81** (2010) 037302 [arXiv:0907.3540 [hep-ph]]; S. Goswami, Nucl. Phys. Proc. Suppl. **188**, 198 (2009); S. Choubey, AIP Conf. Proc. **1405** (2011) 323; M. Blennow and T. Schwetz, arXiv:1203.3388 [hep-ph]; V. Barger, R. Gandhi, P. Ghoshal, S. Goswami, D. Marfatia, S. Prakash, S. K. Raut

and S. U. Sankar, arXiv:1203.6012 [hep-ph].

[8] R. Abbasi *et al.* [IceCube Collaboration], Astropart. Phys. **35**, 615 (2012) [arXiv:1109.6096 [astro-ph.IM]].

[9] O. Mena, I. Mocioiu and S. Razzaque, Phys. Rev. D **78**, 093003 (2008) [arXiv:0803.3044 [hep-ph]].

[10] G. Giordano, O. Mena and I. Mocioiu, Phys. Rev. D **81** (2010) 113008 [arXiv:1004.3519 [hep-ph]].

[11] E. Fernandez-Martinez, G. Giordano, O. Mena and I. Mocioiu, Phys. Rev. D **82**, 093011 (2010) [arXiv:1008.4783 [hep-ph]].

[12] C. H. Ha [for the IceCube Collaboration], arXiv:1201.0801 [hep-ex];
R. Abbasi *et al.* [IceCube Collaboration], arXiv:1111.2731 [astro-ph.IM].

[13] E. K. Akhmedov, M. Maltoni and A. Y. Smirnov, Phys. Rev. Lett. **95** (2005) 211801 [hep-ph/0506064].

[14] E. K. Akhmedov, M. Maltoni and A. Y. Smirnov, JHEP **0705** (2007) 077 [hep-ph/0612285].

[15] E. K. Akhmedov, M. Maltoni and A. Y. Smirnov, JHEP **0806** (2008) 072 [arXiv:0804.1466 [hep-ph]].

[16] D. J. Koskinen, Mod. Phys. Lett. A **26** (2011) 2899.

[17] E. K. Akhmedov, A. Dighe, P. Lipari and A. Y. Smirnov, Nucl. Phys. B **542** (1999) 3 [hep-ph/9808270].

[18] G. L. Fogli, E. Lisi, A. Marrone, D. Montanino, A. Palazzo and A. M. Rotunno, arXiv:1205.5254 [hep-ph].

[19] A. M. Dziewonski and D. L. Anderson, Phys. Earth Planet. Interiors **25** (1981) 297.

[20] D. F. Cowen, D. Grant and J. Koskinen, private communication.

[21] M. Honda, T. Kajita, K. Kasahara and S. Midorikawa, "Calculation of the flux of atmospheric neutrinos," Phys. Rev. D **52**, 4985 (1995) [arXiv:hep-ph/9503439].

[22] J. Conrad, A. de Gouvea, S. Shalgar and J. Spitz, Phys. Rev. D **82**, 093012 (2010) [arXiv:1008.2984 [hep-ph]].

[23] V. Barger, D. Marfatia and K. Whisnant, Phys. Rev. D **65** (2002) 073023 [hep-ph/0112119].

[24] P. Huber and W. Winter, Phys. Rev. D **68** (2003) 037301 [hep-ph/0301257].

[25] A. Y. Smirnov, hep-ph/0610198.

[26] P. Huber, M. Lindner, T. Schwetz and W. Winter, superbeam and reactor experiments,"

JHEP **0911** (2009) 044 [arXiv:0907.1896 [hep-ph]].

[27] G. Fogli, Talk given at the XXV International Conference on Neutrino Physics and Astrophysics, Kyoto, Japan, June 3 - 9, 2012.

http://kds.kek.jp/conferenceTimeTable.py?confId=9151#all.detailed

[28] I. F. M. Albuquerque and G. F. Smoot, Phys. Rev. D **64**, 053008 (2001) [hep-ph/0102078].

[29] H. Minakata, H. Nunokawa and S. J. Parke, AIP Conf. Proc. **670** (2003) 132 [hep-ph/0306221].